UNIVERSITY OF TWENTE.

Faculty of Engineering Technology

The effect of buildings on the morphological development of the beach-dune system

Literature report

Daan W. Poppema, MSc

Jan 2020

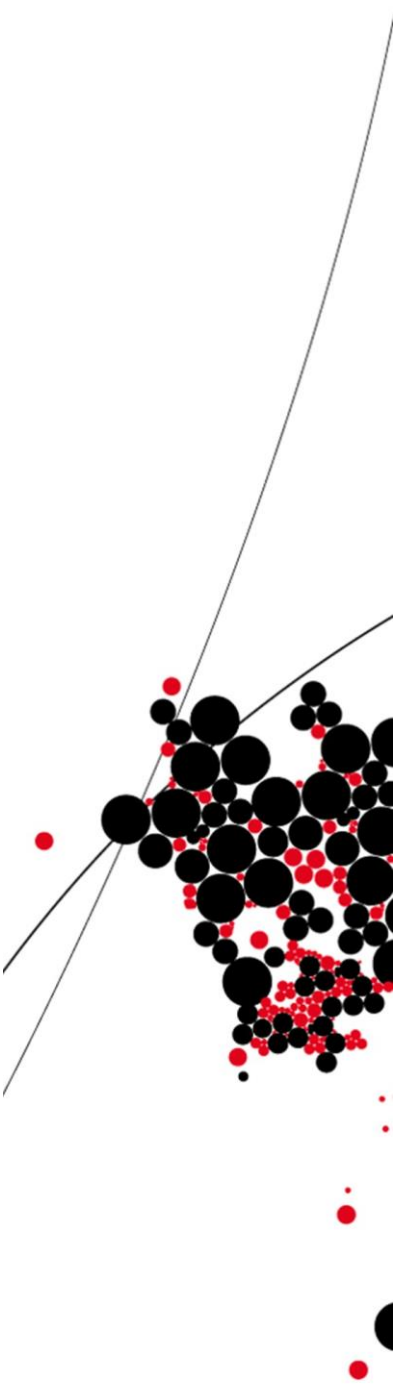

CE&M Research report 2020R-001/WEM-001
ISSN 1568-4652

Literature report:

THE EFFECT OF BUILDINGS ON THE MORPHOLOGICAL DEVELOPMENT OF THE BEACH-DUNE SYSTEM

Daan W. Poppema, MSc

Jan 2020

Supervisors:

prof. dr. K.M. Wijnberg

prof. dr. S.J.M.H. Hulscher

dr. J.P.M. Mulder

Marine and Fluvial Systems
University of Twente

CE&M Research report 2020R-001/WEM-001

ISSN 1568-4652

CONTENTS

1. Introduction 4
   1.1 Background 4
   1.2 Research questions literature review 5
   1.3 Outline 5
2. Sand transport and morphology of the beach-dune system 6
   2.1 The physics of sand transport 6
      2.1.1 The onset of motion 7
      2.1.2 Towards equilibrium transport 9
      2.1.3 Equilibrium transport 10
   2.2 Factors affecting sediment transport 13
      2.2.1 Sediment availability and characteristics 13
      2.2.2 Environmental factors 13
   2.3 Beach and dune morphology 15
3. The influence of buildings 17
   3.1 Wind flow around buildings 18
   3.2 Morphological effects from building presence 22
      3.2.1 The beach and dunes: scientific literature 22
      3.2.2 The beach and dunes: professional literature 24
      3.2.3 Snow accumulation around buildings 26
   3.3 Morphological effects from building usage 31
      3.3.1 Redistributing and steering deposition 31
      3.3.2 Wrack removal 32
      3.3.3 Walking and driving 33
      3.3.4 Building removal 33
4. Conclusion 34

References 35

1

INTRODUCTION

1.1 BACKGROUND

Worldwide, buildings for both recreation and habitation can be found at the beach and in the dunes. Urban developments can likewise be found adjacent to beaches and dune fields. These buildings include houses for vacation or permanent inhabitation; hotels, restaurants and commercial stalls; bathhouses; buildings for lifeguards and rescue services; and lighthouses (Jackson & Nordstrom, 2011). As the coast is generally attractive for recreation, this is a worldwide phenomenon: it can be found on sandy coasts and barrier islands in the Netherlands (Hoonhout & Waagmeester, 2014; Province of Noord-Holland, 2017), Europe (see e.g. Hernández-Calvento et al., 2014; Smith et al., 2017b for case studies on the Canary Isles), the United States (Nordstrom & McCluskey, 1984; Morton et al., 1994; Feagin et al., 2010), and also in more developing countries (e.g. Ranieri, 2014 for Salinópolis, Brasil). In the Netherlands, there is an increasing demand for these buildings and a shift to a stronger year-round presence (Hoonhout & Waagmeester, 2014; Province of Noord-Holland, 2017). A similar growth in coastal tourism in general (Hall, 2001; Moreno & Amelung, 2009) and the number of buildings at the beach (Schlacher et al., 2008; Malavasi et al., 2013) can be found in other countries.

All these buildings affect the wind field and wind-driven sediment transport in their surroundings (Nordstrom & McCluskey, 1984; Nordstrom, 2000; Jackson & Nordstrom, 2011; Smith et al., 2017b). Further effects are introduced as unintended by-product from building usage (e.g. trampling of vegetation and changes to surface roughness caused by walking and driving, see Andersen, 1995; Jackson & Nordstrom, 2011) and as result of building owners actively shaping the environment (e.g. removing sediment deposits on paths and terraces, see Nordstrom et al., 1986). Through these effects, buildings can influence the morphology of their direct surroundings and the larger beach-dune system.

Aeolian sediment transport from the beach zone to the dunes is important for an ecologically healthy dune system: rare and valuable vegetation species thrive under a regime with a sand influx - with the optimal sedimentation or erosion regime depending on the species (Van der Putten et al., 1993; Hoonhout & Van Thiel de Vries, 2013). From the perspective of water safety, the same landward sediment flux is important for long-term coastal safety. Dunes protect developments both on the dunes and in the hinterland behind the dunes against flooding. The influx of sand is needed to balance natural storm-induced dune erosion (Morton et al., 1994; Keijsers, 2015) and to let dunes keep step with (relative) sea-level rise and compensate for the expected increase in hydrodynamic erosion (Carter, 1991; Keijsers, 2015; De Winter & Ruessink, 2017).

The combination of (1) a worldwide presence and demand for buildings at the beach-dune interface, (2) their effect on the Aeolian sediment transport and beach-dune morphology and (3) the importance of Aeolian sediment transport for both ecology and coastal safety necessitate a proper understanding of how buildings on the beach-dune interface affect their environment. This is of great interest to water managers and regional authorities that have to decide if – and in what form – this kind of developments is allowed and they would like to have well-founded rules on the allowance criteria for buildings in the coastal zone.

1.2 RESEARCH QUESTIONS LITERATURE REVIEW

This literature review serves as the starting point of a PhD research into the effect of the presence and usage of configurations of buildings at the beach-dune interface on Aeolian sediment transport and long-term dune development. Two main research questions will be answered in this literature review:

1. *Which factors determine the sand transport and morphological development of the beach-dune system?*
   As a first step, the physics and factors affecting sediment transport and morphology on a natural beach-dune system are described. With this knowledge, changes induced by buildings can be better distinguished and understood. Special interest here is paid to the physics and scaling of sediment transport, in order to better understand and interpret scaled field experiments that are conducted during the PhD.
2. *What is currently known of the influence of the built environment on the beach-dune system?*
   Here, the current knowledge on the influence of buildings on the beach-dune system is examined and gaps in our knowledge are identified.

Literature has mainly been found by following references from key articles. In addition, Scopus has been used to identify relevant articles less often cited in other articles.

1.3 OUTLINE

In chapter 2, general sand transport and morphology of the beach-dune system are examined. First the physics of sand transport are explained (section 2.1), followed by factors affecting sediment transport (2.2) and a description how gradients in sediment transport over time form the beach-dune morphology (2.3). Then, chapter **Error! Reference source not found.** focuses o n buildings and the effects they have. Section 3.1 starts with the wind flow around buildings, followed by the state of the art of the morphological effects from the *presence* of buildings (3.2) and *usage* of buildings (3.3).

2

SAND TRANSPORT AND MORPHOLOGY OF THE BEACH-DUNE SYSTEM

The beach and the dune are dynamic systems, with changes occurring both on short timescales (e.g. seconds to minutes) to long timescales (years or decades). In this chapter, the state-of-the-art knowledge on beach-dune dynamics will be described. It starts with the physics of sediment transport (section 2.1) and factors affecting sediment transport (section 2.2). Section 2.3 continues with beach-dune morphology. The distinction between sediment transport and morphology is important as they both relate to different time scales: morphological change depends on long-term trends in sediment transport. More specifically, it is the result of an average spatial convergence or divergence in the sediment transport over a longer period of time.

2.1 THE PHYSICS OF SAND TRANSPORT

Sediment transport occurs when the destabilizing forces on a particle exceed the stabilizing forces. The destabilizing force generally comes from water movement for hydrodynamic transport or air movement for Aeolian transport. Although the physics are the same for both, the difference in density leads to marked differences in the observed transport. Apart from the environment, several modes of transport can be distinguished (Bagnold, 1941; Kok et al., 2012), as visible in Figure 1. Bedload transport occurs when particles are large and flow velocities small. Once dislodged by drag force, grains roll or slide over the surface. This is called *tractation* or creep motion. In this regime, hydrodynamic (or aerodynamic) forces, gravity and contact forces are all important. Conversely, when particles are fine and flow velocities are large, hydrodynamic forces dominate and particles move in *suspension*. In the intermittent regime, tractating particles lift off from the bed due to hydrodynamic lift force or bumps in the surface, upon which gravity pulls them back down. This movement in successive jumps is called *saltation*. When saltating particles collide with the bed with sufficient energy, new particles are ejected and make a short jump. This mode, called *reptation*, is exclusive to Aeolian transport: water and other dense fluids dissipate the kinetic energy needed to expel new grains.

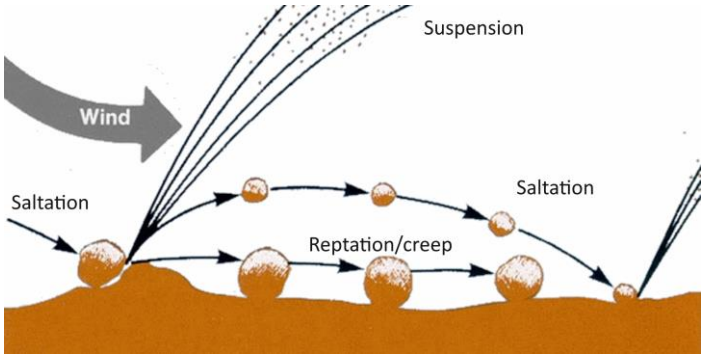

Figure 1: A schematic representation of the transport modes in Aeolian transport (adapted from NASA, 2002)

2.1.1 THE ONSET OF MOTION

Sediment starts to move when the destabilizing force exceeds the stabilizing force. This occurs when the drag force exerted by water or air motion exceeds the friction force. To compare these forces, the Shields number (originally Shields, 1936; Durán et al., 2011; Kok et al., 2012) can be used (Θ, see eq. 2.1, with τ bed shear stress, ρ density, g the gravitational constant, d grain diameter and subscripts p and f for particle and fluid). The Shields number is a nondimensionalization of the shear stress. Its meaning becomes clear by multiplying the numerator and denominator of the fraction with d^2 (eq. 2.2, with u_* the shear velocity). The numerator, so the bed shear stress times the frontal area of a particle, is proportional to the drag force on a grain, with the exact proportionality depending on the drag coefficient (particle shape), velocity profile and the part of the grain exposed to the flow (Durán et al., 2011; Kok et al., 2012). The denominator, so net particle weight, expresses the contact force between grains and is proportional to the friction between grains.

$$\Theta = \frac{\tau}{(\rho_p - \rho_f)gd} \tag{2.1}$$

$$\Theta = \frac{\rho_f u_*^2 * d^2}{(\rho_p - \rho_f)gd^3} \tag{2.2}$$

The Shields number at which sediment start moving is called the critical Shields number. Alternatively, the expression can be rewritten to derive the critical shear velocity u_{*cr} at with grains starts moving (eq. 2.3). This is also the expression that Bagnold (1941) used, although he used a fluid threshold A_t for $\sqrt{\Theta_{cr}}$.

$$u_{*cr} = A_t \sqrt{\frac{(\rho_p - \rho_f)}{\rho_f} gd} \tag{2.3}$$

The critical shields number (or fluid threshold) depends on both particle properties and environmental properties. The main factors are the Reynolds number (turbulent intensity), the friction (coefficient) between particles, the presence of cohesion, fluid viscosity and the lift force (a small upward force caused by the lower pressure above a particle than below it, originating from the velocity gradient and Bernoulli principle) (Kok et al., 2012). Furthermore, a distinction has to be made between the static and dynamic critical Shields number (Durán et al., 2011; Kok et al., 2012). The static number indicates at which shear stress particles start moving, the dynamic number indicates when particle movement can be sustained. The difference is caused by the splash process, in which saltating particles hitting the ground transfer momentum to static particles, thereby triggering particle movement. This is also visible in Figure 2, in which the static and dynamic critical shields number are plotted for both hydrodynamic and Aeolian experiments.

The critical shields number and shear velocity increase strongly for decreasing particle size, due to interparticle forces (cohesion). This is also visible in Figure 2 and Figure 3. The Bagnold equation, so eq. 2.3 (with $A_t \approx 0.10$) does not take interparticle forces into account. However, several semi-empirical expressions do, a number of which are plotted in Figure 3. Iversen and White (1982) related the threshold parameter A_t explicitly to the Reynolds number, particle

size, particle density and viscosity (see Iversen & White (1982) or Kok et al. (2012) for the complete expression). Shao and Lu (2000) have severely simplified this relation, based on the limited effect of the Reynolds number and the relation between particle diameter and interparticle force. As the interparticle force scales approximately linear with particle diameter (see also Kok et al., 2012), they account for cohesion by adding a term γd to eq. 2.2, with γ being a constant. This results in eq. 2.4. Figure 3 shows that this expression fits experimental results quite well. Alternatively, Claudin and Andreotti (2006) scale the interparticle forces with $d^{4/3}$ instead of d, leading to slightly different expressions.

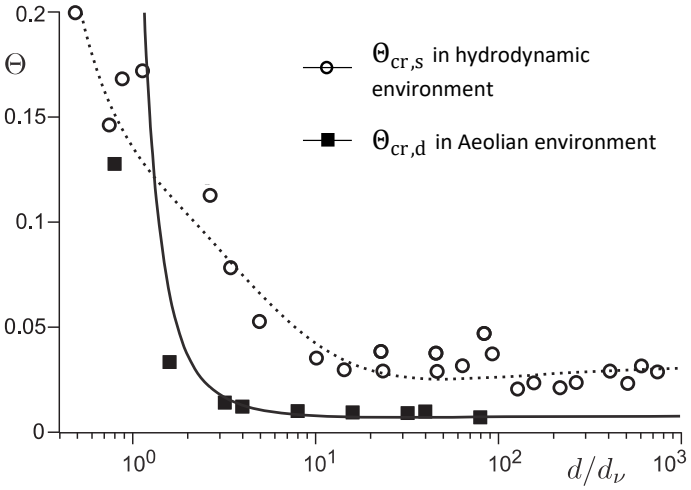

Figure 2: A graph of the static and dynamic critical shields number against grain size d, rescaled by the viscous diameter $d_v = (\rho_p/\rho_f - 1)^{-1/3} \nu^{2/3} g^{-1/3}$. Figure adapted from Fig. 15a from Durán et al. (2011), based on data from Fernandez Luque and Van Beek (1976); Yalin and Karahan (1979) for $\Theta_{cr,s}$ and Chepil (1945b, 1945a, 1945c), and (Hsu, 1971) for $\Theta_{cr,d}$.

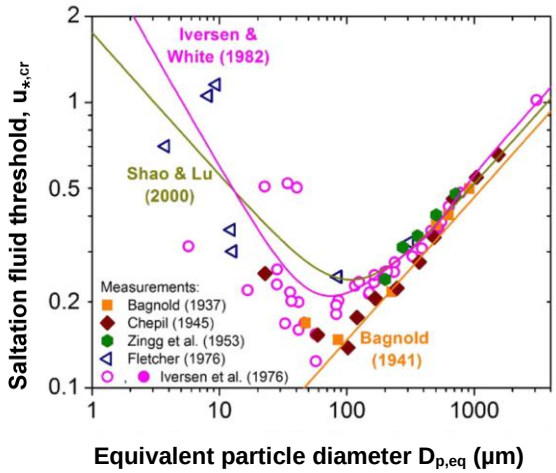

Figure 3 Semi-empirical expressions (coloured lines) and measurements (symbols) of the threshold shear velocity. Measurements for sand and dust are denoted by filled symbols, measurements on other materials by open symbols. The effect of material density differences on the fluid threshold was accounted for using an equivalent diameter $d_{p,eq} = d\,\rho_p/\rho_{sand}$. The Bagnold expression is given in eq. 2.3, the Shao & Lu expression in eq. 2.4. For the Iversen & White expression, see Iversen and White (1982). Figure adapted from fig. 5 in Kok et al. (2012).

$$u_{*,cr} = A_t \sqrt{\frac{(\rho_p - \rho_f)}{\rho_f} g d + \frac{\gamma}{\rho_f d}} \qquad (2.4)$$

2.1.2 TOWARDS EQUILIBRIUM TRANSPORT

After the onset of motion, the evolution to equilibrium transport consists of two phases. Phase 1 is an increase in the sediment concentration, followed by an increase in the average particle velocity (Durán et al., 2011). The increase in the sediment concentration occurs mostly by splash: the ejection of new particles by saltating grains colliding with the bed. The velocity of newly ejected particles is typically an order of magnitude lower than that of incoming particles (Rice et al., 1996) because incoming particles themselves can also rebound, incoming particles can eject multiple particles and momentum is transferred to the bed (Kok et al., 2012). Consequently, most splashed particles are in the low-energy reptation regime, and only make small hops. However, when these particles are sufficiently accelerated by the wind, they can (after several hops) splash new particles. This leads to an exponential increase in the particle concentration. Simultaneously, the transfer of momentum from the wind to particles decreases the wind velocity. This continues until a steady state is reached, in which on average exactly one particle leaves the surface (by rebound or ejection) for every particle colliding with the surface.

The increase in the sediment concentration and in the sediment velocity can be distinguished as separate phases in sediment flux experiments. Figure 4 shows the spatial variation of the sediment flux over a flat sand bed. Initially, the sediment concentration increases exponentially. This increase can be characterized by an ejection length, $L_{1/4}$, the length it takes to reach a flux that is ¼ of the equilibrium flux. Figure 5 shows that $L_{1/4}$ depends strongly on the wind shear velocity, indicating that the replacement capacity is higher at higher wind speeds. After this phase, the flux exhibits relaxation to equilibrium. This relaxation is characterized by the saturation length L_{sat}, (see eq. 2.5). Figure 5 shows that the saturation length is quite independent of the wind shear velocity. Durán et al. (2011) demonstrated that the saturation length can be estimated with eq. 2.6, based on a physical analysis of the acceleration of inertial particles experiencing a drag force and on a stability analysis of the wavelengths of dune formation. For parameter α in eq. 2.6 they used a value of order 2 (Andreotti, 2004), resulting in a saturation length of approximately 1 meter for Aeolian transport (using d=200 μm). However, using a similar set-up, Shao and Raupach (1992) found no distinctive splash phase and larger saturation lengths (see also Fig. 4 in Shao & Raupach, 1992). Furthermore, they found that especially for larger particles the sediment flux overshoots the equilibrium value, due to the deceleration of the wind and the response time of particles to the wind speed.

$$q = \alpha \cdot \left(1 - e^{-\frac{x - x_0}{L_{sat}}}\right) \tag{2.5}$$

$$L_{sat} \approx 2\frac{\rho_p}{\rho_f} d \tag{2.6}$$

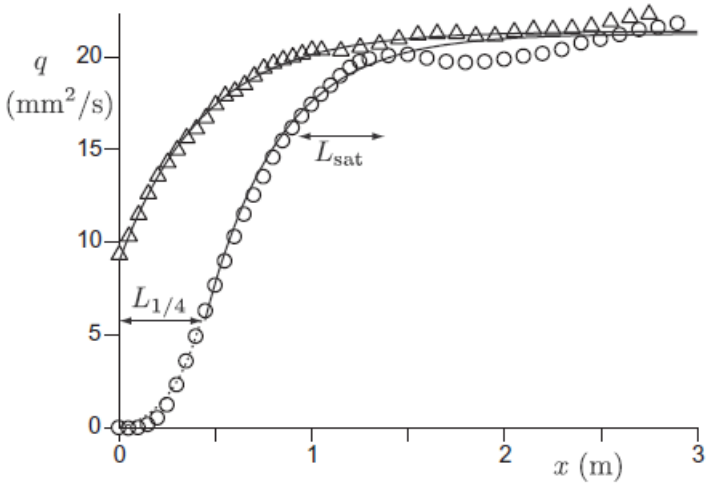

Figure 4 The spatial variation of the sediment flux q over a flat sand bed in a wind flume (adapted from fig. 1 in Andreotti et al., 2010). The experiment is performed with (△) or without (□) an input flux, at $u_* = 0.33\ m/s \approx 1.5u_{*,cr}$ and with a grain size of 120 μm. The dotted line show the initial exponential increase up to ¼ of the saturated flux, the solid lines show the best exponential fit around the saturated state. The ejection length $L_{1/4}$ is the length needed before the flux q reaches $q_{sat}/4$; the saturation length L_{sat} is the relaxation length close to the saturated state.

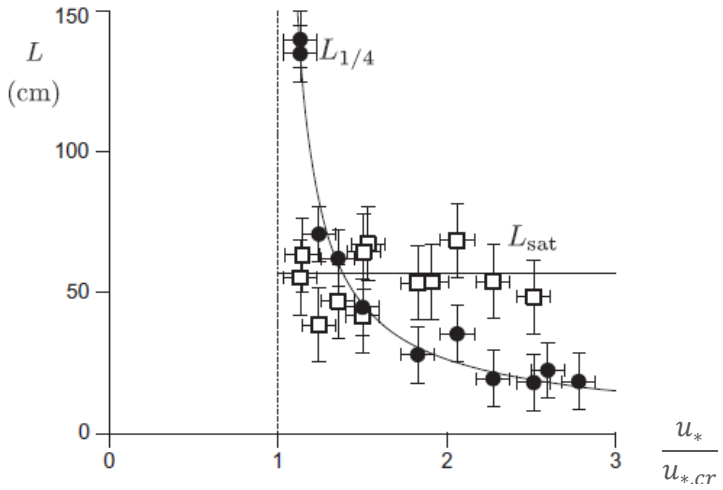

Figure 5: Measurements of ejection length $L_{1/4}$ (circles) and the saturation length L_{sat} (squares) as a function of the wind shear velocity u_*, rescaled by the (dynamic) critical shear velocity $u_{*,cr}$. The solid lines show the best fit by a power law and a constant. The figure shows that $L_{1/4}$ decreases with increasing wind speed, while L_{sat} is approximately constant. (adapted from fig. 3 in Andreotti et al., 2010)

2.1.3 EQUILIBRIUM TRANSPORT

In order to generate sediment movement (transport), momentum has to be transferred from the air to the particles. This leads to the occurrence of a transport layer, in which sediment is transported and the air velocity is lower. If the transport is in equilibrium, the average replacement factor is one: particles colliding with the bed generate on average one saltating particle. The replacement capacity depends on the drag force exerted on particles at the bed and on the kinetic energy of colliding particles (Durán et al., 2011; Kok et al., 2012). Therefore, the equilibrium wind (shear) velocity and particle velocity in the transport layer close to the bed are fairly constant, i.e. they do not depend on the undisturbed wind shear velocity u_* (Ungar & Haff, 1987). Consequently, the average hop length, which depends on the velocity of the particles and the wind speed, is also fairly independent of u_*.

This is supported by both wind tunnel experiments (Figure 6a,b) and simulations (Figure 6c), which show that the wind speed at a height of approximately 1 cm above the surface is independent of the wind shear velocity. This intersection point of the velocity profiles is called the Bagnold focus. As a result of the similar wind velocities, the velocity of particles moving close to the bed is also fairly independent of the wind shear velocity (Figure 6d-f). However, the velocity of high energy particles moving above the Bagnold focus scales with u∗. Consequently, the probability function of particle speeds widens with increasing u_* (Figure 7).

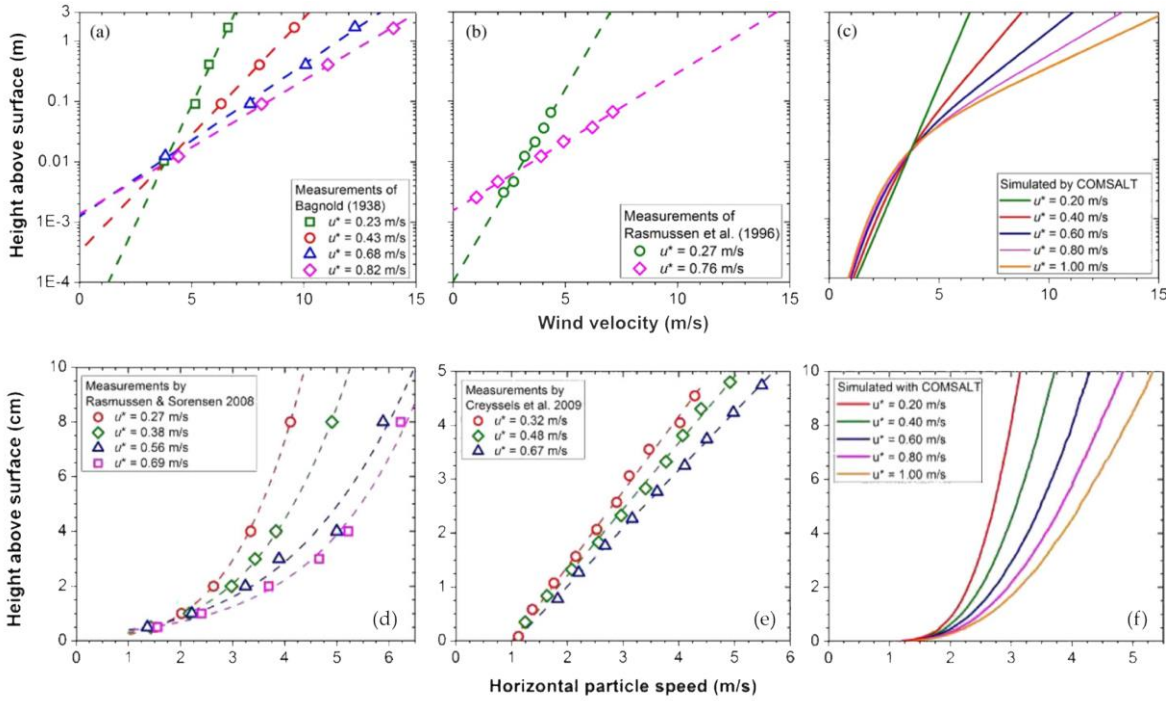

Figure 6: The wind velocity (a-c) and particle velocity (d-f) in measurements and models of Aeolian transport. Subplot a-c show the occurrence of the Bagnold focus, where the wind shear velocity is independent of the undisturbed wind velocity. Subplot d-f show that the particle velocity close to the bed is almost independent of the undisturbed shear velocity. N.b. The y-axis of subplot a-c is in m, of subplot d-f in cm. Adapted from fig. 12 and 14 in Kok et al. (2012).

Based on this information, an equation for the mass flux as a function of the wind shear velocity can be derived (Kok et al., 2012). In the generation of sediment transport, the momentum of the wind is partly absorbed by particles in the saltation layer. By momentum balance, the (undisturbed) shear stress τ on top of the transport layer is equal to the shear stress at the surface by particles (τ_p) and air (τ_a) (eq. 2.7). A common assumption is that the shear velocity in the transport layer is equal to the threshold shear velocity ($u_{*,t}$), based on the fact that the replacement capacity is exactly 1 (eq. 2.8).

$$\tau = \tau_p + \tau_a \qquad (2.7)$$

$$\tau_p = \tau - \tau_a \approx \rho_a u_*^2 - \rho_a u_{*,t}^2 \qquad (2.8)$$

By Newton's second law, the shear stress on the particles is equal to the momentum extracted by the particles (eq. 2.9, with M the mass per m^2 of the particles in motion, a the acceleration of the particles and Δu_p the average difference in horizontal velocity between particle landing and lift-off.

$$\tau_p = Ma = M\frac{\Delta u_p}{T_{hop}} \tag{2.9}$$

Sediment transport is a function of the velocity and mass of the particles in motion (eq. 2.10). Using eq. 2.8 and 2.9, this can be expressed in the shear velocities of the flow, resulting in eq. 2.11:

$$Q = Mu_p = M\frac{L_{hop}}{T_{hop}} \tag{2.10}$$

$$Q = \frac{M}{T_{hop}}L_{hop} = \frac{\tau_p}{\Delta u_p}L_{hop} = \rho_a\left(u_*^2 - u_{*,t}^2\right)\frac{L_{hop}}{\Delta u_p} \tag{2.11}$$

Based on different assumptions on how the hop length, particle velocity (and shear velocity at the surface) depend on the u_*, many different expressions for the equilibrium sediment flux have been coined (see e.g. table 1 in Kok et al., 2012). Bagnold (1941) originally proposed the particle velocity to scale with u_*, resulting in a cubic relation between wind velocity and sediment transport. In contrast, more recent research (Ungar & Haff, 1987; Kok et al., 2012 and references therein) argue for quadratic scaling, based on a fairly constant particle speed (i.e. independent of u_*).

However, the wind speed in higher layers is not constant. Therefore, particle velocity in these layers also increases with u_*. These particles form an increasing fraction of the whole transport (see Figure 7). Consequently, the average particle velocity is no longer constant at higher wind velocities. This has lead Durán et al. (2011) to the definition of a change from quadratic to cubic scaling at higher wind velocities (more than approximately 5 times $u_{*,t}$).

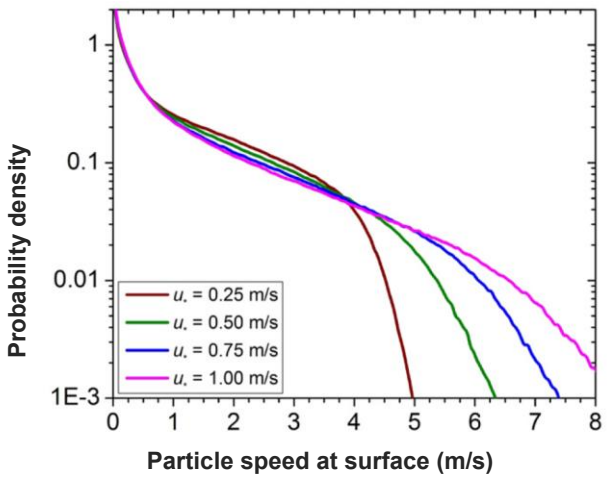

Figure 7 The horizontal particle speed distribution at the surface shows that with increasing shear velocity (u_*), the right-hand tail increases, meaning the portion of particles with a high velocity increases. The particle speed distribution is based on numerical simulations of the velocity of 250 µm particles (figure adapted from fig. 16 in Kok et al., 2012).

2.2 FACTORS AFFECTING SEDIMENT TRANSPORT

The previous section describes the physics behind (Aeolian) sediment transport, eventually leading to general expressions to predict the sediment flux. Important parameters pinpointed by these expressions are the wind (shear) velocity and the threshold shear velocity of particles. Especially the threshold shear velocity depends on many underlying factors, of which the grain size and grain size distribution were the most important. However, there are many more variations in the environment that affect the sediment flux. Moreover, the described sediment flux is actually a sediment flux potential. In other words: the aforementioned expressions assume transport-limited conditions, in case of a limited sediment supply the amount of sediment transport will be lower. This section will explain these factors in more detail.

2.2.1 SEDIMENT AVAILABILITY AND CHARACTERISTICS

The previous section identified the threshold shear velocity as an important factor in sediment transport. The effect of grain size is already extensively discussed in section 2.1 (see figure 2 and 3). However, the grain size distribution also plays a role. With a wider grain size distribution, the critical shear stress of the smallest grains becomes smaller (Nickling, 1988). This can increase the sediment transport rate (Bagnold, 1941; Horikawa et al., 1983). However, a wider distribution can also decrease the transport rate when larger particles armour the underlying bed (Van der Wal, 1998; Hoonhout, 2017).

Van der Wal (1998) examined the effect of the wider grain size distribution on nourished beaches in the Netherlands and found that shells and other large particles formed an erosion-resistant layer on the bed. This armouring of the erodible sediments decreased sediment transport rates. The results of Hoonhout (2017), who examined armouring at the Sand Motor mega nourishment, support these findings. Within a year after construction of the Sand Motor, shells and other large particles had formed an armour layer. Due to the high elevation of the Sand Motor, waves were unable to reach and rework this layer. Consequently, sand from the intertidal beach formed the majority of the sand transport. This sand was deposited temporarily in the higher areas before it was transported further. Given that the sand transport at the Sand Motor is determined by the influx from the intertidal zone, this basically means transport is supply-limited instead of transport-limited.

2.2.2 ENVIRONMENTAL FACTORS

The sediment characteristics and momentaneous wind conditions determine the theoretical equilibrium transport. However, environmental factors like spatial and temporal variations in wind (shear) stress, geometry, slope, vegetation cover and soil water content determine if this equilibrium transport is reached. Due to the time and thereby distance needed to reach equilibrium, this is seldom the case (Bauer et al., 2009).

The geometry of the beach determines the distance over which sediment can be picked up. This distance, called the fetch distance, depends on the beach width and wind direction (see Figure 8 for a sketch and Delgado-Fernandez (2010) for a review on the fetch length). If the fetch length is shorter than the critical fetch length, the transport does not reach equilibrium. However, estimates for the critical fetch length vary wildly: wind tunnel measurements can be as low as a few metres, while field studies range from tens to hundreds of metres (Delgado-Fernandez, 2010). This difference has several reasons. The compressed vertical profile found

in wind tunnels may accelerate the development of an equilibrium concentration (Bauer et al., 2004). Furthermore, Dong et al. (2002; 2004) found a positive relationship between wind velocity and fetch length. In combination with the generally relatively low velocities of wind tunnels, this would lead to an underestimation from wind tunnels (Delgado-Fernandez, 2010). However, note that Durán et al. (2011) only found the ejection length ($L_{1/4}$) to depend on wind shear velocity, not the saturation length (see also Figure 5). A further explanation for the difference is that field conditions can be supply-limited (Delgado-Fernandez, 2010). The aforementioned armouring (Hoonhout, 2017) can for instance limit sediment pick-up, thereby increasing the distance needed to reach full sediment transport.

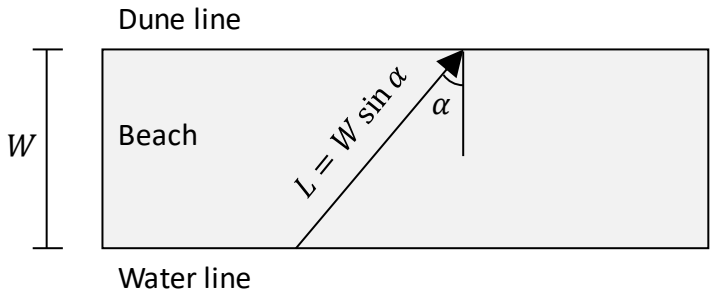

Figure 8 A sketch of the fetch length (L) as a function of beach width (W) and wind angle (α).

The water content of the sediment can also have a strongly limiting effect on sediment transport (Duarte-Campos et al., 2018). This can be explained by increasing cohesion and increasing critical shear velocity (Namikas & Sherman, 1995; Davidson-Arnott et al., 2007; Bauer et al., 2009). However, a quantification of the effect is very difficult (Namikas & Sherman, 1995). One difficulty is that the effect is less pronounced during very high wind conditions, when even moist sediment is can be transported (Bauer et al., 2009). Additionally, Bauer et al. (2009) note the role of spatial and temporal variations in surface moisture contents. Dry sand layers can be episodically stripped from the beach in the form of streamers (Williams et al., 2018), after which the underlying moist sediment needs an extended period of time to dry before it is suddenly transported again.

The water content of the beach depends on a whole range of factors. The elevation and tidal excursion determine the location of the intertidal zone and the frequency and duration of flooding. The elevation, slope and wave conditions determine the extent of the wave run-up. The topography and the porosity of the soil determine the groundwater flows (e.g. from the dunes to the lower-lying beach). The weather supplies rainfall, but the temperature and wind also affect the drying of the beach. Furthermore, barometric pressure changes caused by the weather system have been related to variations in the groundwater table (Namikas & Sherman, 1995; Horn, 2002; Davidson-Arnott et al., 2007; Bauer et al., 2009).

Many of the factors described before come together in beach nourishments, which gives them a profound effect on Aeolian sediment transport. According to Jackson and Nordstrom (2011, p. 184), this effect is the result of: "(1) an increase in source width for entrainment of sediments; (2) changes in grain size characteristics that affect the likelihood of entrainment and transport; (3) changes in moisture conditions due to increased elevation; (4) changes in the shape of the beach or dune profile; and (5) changes in the likelihood of marine erosion of the foredune".

2.3 BEACH AND DUNE MORPHOLOGY

The previous section describes factors affecting the sediment transport rate. By mass balance, a spatial or temporal gradient in sand transport will result in erosion or deposition, and thereby change the elevation. So the highly variable nature of Aeolian sand transport leads by definition to short-term elevation changes. Over time, trends in Aeolian transport can also lead to long-term elevation changes and the emergence of spatial structures. These trends in the Aeolian transport can for instance be caused by spatial variations in the beach structure (bedforms), elements present on the beach (e.g. vegetation or wrack) or human actions (grazing, mowing, and cleaning). These factors affecting the long-term evolution of the beach-dune system are examined in this section.

Vegetation at the beach disturbs the wind field and sediment transport (Hesp, 1989; Van Puijenbroek et al., 2017). The wind is slowed down and behind vegetation, a shadow zone with increased sedimentation occurs. Furthermore, the vegetation canopy can trap sediment, while roots stabilize the bed and decrease the erodibility. The resulting sedimentation inside and behind vegetation can form the starting point for embryonal dune formation. For existing dunes, vegetation can increase the sedimentation rate and decrease dune mobility (i.e. fix them in place, see Durán & Herrmann, 2006).

Vegetation depends on freshwater availability, so soil moisture and precipitation have a positive effect, while salinity and salt spray have a negative effect on vegetation (Hesp, 1989; Van Puijenbroek, 2017). Furthermore, the sedimentation rate affects the establishment and growth of plants. Pioneer species often thrive under sedimentation (Gilbert et al., 2008; Van Puijenbroek, 2017). This positive feedback between sedimentation and plant growth allows dunes to grow, at which point their shape starts directly affecting sediment transport (Van Puijenbroek, 2017).

Other objects present at the beach, such as rocks, wrack or garbage, can play a similar role, slowing down wind and causing sedimentation in their shadow zone (Hesp, 1989; Van Puijenbroek, 2017). As lifeless objects, these miss the positive feedback loop and the ability to keep up with sedimentation. However, wrack does contain seeds, rhizomes and nutrients of coastal vegetation and nutrients that can form the starting point of vegetation (Jackson & Nordstrom, 2011; Van Puijenbroek, 2017). Furthermore, the wrack line can function as a sediment trap to cross-shore sediment transport (Jackson & Nordstrom, 2011).

Apart from these elements present on the beach, the shape of the beach itself also affects the wind field and sediment transport. Bedforms (dunes and ripples) affect the wind velocity, turbulent intensity, streamline curvature and bed shear stress (Livingstone et al., 2007; Smith et al., 2017a). Effects on the flow structure include flow deceleration at the dune toe, flow acceleration and compression along the stoss side of the dune, flow detachment at the crest, flow deceleration and recirculation at the leeward side and finally flow reattachment further downwind of the dune (Smith et al., 2017a and references therein). Although these features can individually both increase and decrease sediment transport, their combination leads generally to erosion of the stoss side of a dune, and deposition in the shadow zone behind the dune (see Figure 9 and Wiggs et al., 1996). As a result, dunes tend to migrate in the (dominant) wind direction. These processes are similar to the sand transport and migration of river dunes (Hulscher & Dohmen-Janssen, 2005). Based on these similarities, aeolian dunes have been studied using subaqueous experiments, e.g. to examine the migration speed of barchan dunes (Hersen, 2005).

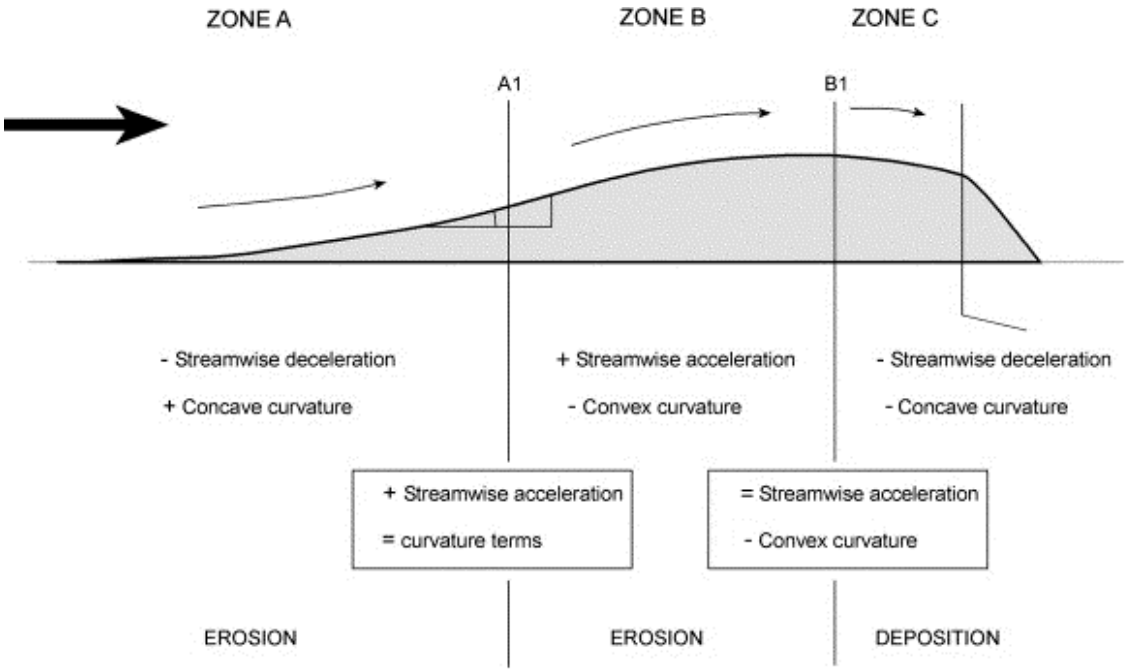

Figure 9: A schematic representation of dune dynamics, based on the notion that flow acceleration and concave streamline curvature increase bed shear stress and erosion (indicated by plus signs), while flow deceleration and convex curvature promote deposition (indicated with a minus) (adapted from Wiggs et al., 1996, fig. 18). Zone A: Upwind of a dune flow is decelerated due to the mass of the dune and the adverse (increasing) pressure gradient. Streamlines are curved concavely as a response to the deflection of wind over a dune. At point A1 the slope transitions from concave to convex. So streamline curvature has no effect on the shear stress. With flow acceleration at its maximum here, strong erosion occurs. In zone B, streamwise acceleration decreases from its maximum in point A1, while the convex slope and hence convex streamline curvature increasingly suppress erosion. So the erosion gradually decreases, until at the crest (B1) deposition becomes dominant. In zone C, flow deceleration and convex curvature both cause deposition between the dune crest and the brink of the dune. Downwind of the dune, flow detachment and recirculation cause sedimentation.

3

THE INFLUENCE OF BUILDINGS

This chapter examines the current knowledge on the effect of buildings on wind flow, sediment transport, and beach-dune morphology. Section 3.1 starts with the wind velocity and flow structures around buildings. Next, research into effects from the presence (section 3.2) and usage (section 3.3) of buildings on sediment transport and morphology are presented.

Buildings spatially replace the beach or dune and thereby reduce the source area for windblown sediment transport (Morton et al., 1994; García Romero et al., 2016) and alter the wind direction and wind speed in their surroundings (Nordstrom & McCluskey, 1984; Jackson & Nordstrom, 2011; Smith et al., 2017b). They can decrease the wind speed and promote sedimentation in their surroundings, for instance in front of and at the lee side of buildings (Nordstrom, 2000; Jackson & Nordstrom, 2011; Smith et al., 2017b). Conversely, air flow in between buildings can also be accelerated, causing local erosion and increased sediment transport (Nordstrom, 2000; Jackson & Nordstrom, 2011). The same effect can be seen under houses on pilings, where a scour zone can commonly be found (Nordstrom & McCluskey, 1984; Nordstrom & James, 1985; Jackson & Nordstrom, 2011). Especially continuous lines of buildings can form a barrier against sediment transport, detaching dunes from their beach or foredune sources and thereby causing fetch segmentation (Jackson & Nordstrom, 2011; Smith et al., 2017b). Furthermore, an increased turbulent intensity in the wake of houses can promote an increase in sediment transport (Smith et al., 2017b). Sunlight blockage by houses can reduce the growth of stabilizing dune vegetation (Nordstrom & McCluskey, 1984).

The effect that buildings have on their environment depends on the properties of the building and the environment: the building size, shape, material and location; the distance between buildings; the orientation with respect to the wind direction and coastline; and the time and duration that a building is present (Nordstrom, 2000; Jackson & Nordstrom, 2011).

- The size determines the size of the affected area, the reduction of the source area for windblown sediment transport and the degree to which a (high rise) building rises into the atmospheric boundary layer (Jackson & Nordstrom, 2011; Smith et al., 2017b).
- The shape determines how wind, sediment, and bedforms can move around, over and (in case of elevated buildings) under a building (Jackson & Nordstrom, 2011). In addition, shape determines if flow separation occurs at sharp corners (Nordstrom & McCluskey, 1984).
- Building material determines the hardness and elasticity of the surface and the degree to which the momentum of particles colliding with the structure is absorbed (Durán et al., 2011; Jackson & Nordstrom, 2011). In addition, building roughness affects the velocity profile of wind in the boundary layer with the building, akin to roughness and roughness elements at the bed (Taylor, 1969).
- Location determines the degree to which buildings cause fetch segmentation and the degree to which buildings are also exposed to wave attack and hydrodynamic erosion

(Jackson & Nordstrom, 2011). Furthermore, it determines the potential for interactions between the building's effects (on wind flow, sediment transport and morphology) and other features (e.g. dunes, bedforms or vegetation) (Nordstrom & McCluskey, 1984).

- The distance between buildings determines whether wind in between buildings is accelerated or decelerated and the degree to which buildings form a barrier to sand transport (Nordstrom & McCluskey, 1984; Hoonhout & Van Thiel de Vries, 2013).
- The orientation with respect to coastline affects the speed with which sand can accumulate around buildings. The fetch distance and sediment transport rate are larger for shore-parallel wind directions (Bauer et al., 2009; Delgado-Fernandez, 2010). Consequently, structures with the long axis perpendicular to the coast can trap sediment at a faster rate (Jackson & Nordstrom, 2011).
- The orientation with respect to the wind determines the type of flow structures around a building (Castro & Robins, 1977; Peterka et al., 1985), thereby affecting the sedimentation and erosion patterns (Liu et al., 2018).
- The time and duration of building placement (so summer placement versus permanent placement) determine the effects and processes in winter. For year-round placement, effects continue building up in winter. For summer placement, there is no winter effect, and already formed deposition patterns can be partially eliminated.

3.1 WIND FLOW AROUND BUILDINGS

Buildings affect the wind in their surroundings and create complicated airflow patterns. In general, an object in a flow will diverge the flow around and over the object. In case of buildings, the turbulence of the wind and the bluff nature of most buildings also create a highly turbulent wake behind the building (Hunt, 1971; Fackrell, 1984; Peterka et al., 1985). Assuming a simple cubic shape oriented perpendicular to the wind, Figure 10 shows the mean wind flow pattern around this building.

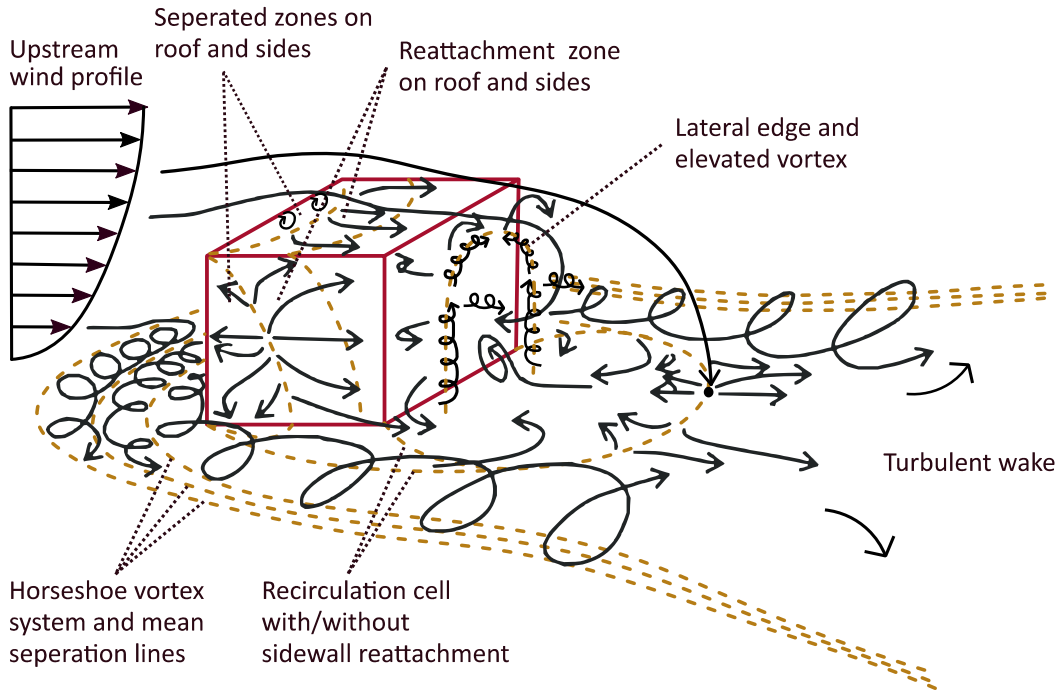

Figure 10: The mean streamline patterns around a building oriented perpendicular to the wind, modified from Hunt et al. (1978) and Blocken et al. (2011).

Flow approaching a building is diverted around it (see Figure 10). A stagnation zone exists around ⅔ to ¾ of the building height. Above this zone, the wind is diverted upward and to the sides. Below this zone, the pressure caused by the wind profile diverts the wind downward and to the sides (Peterka et al., 1985). The flow to the sides and top of the building front separate from the building at the front edges (Hunt, 1971; Peterka et al., 1985). Furthermore, the increased pressure and downward flow upwind of the building cause a reverse flow close to the ground. This creates a rotating vortex with flow separation in front of the building, that is wrapped around the building in a horseshoe shape (Hunt, 1971; Peterka et al., 1985). Smaller vortices in front of the building are entrained in the horseshoe vortex. A consequence of this flow structure is that wind speeds that are normally found at 2/3 to ¾ of the building height are effectively brought to the surface, increasing local wind speeds (Peterka et al., 1985).

The separated flow over the building edges can reattach at the top and side of the building before it reaches the back of the building. This depends on the building's length-to-width and length-to height ratio (Hunt, 1971; Wilson, 1979; Peterka et al., 1985) and the turbulent intensity (Hunt, 1971; Castro & Robins, 1977; Fackrell, 1984; Peterka et al., 1985) – with a larger upwind roughness and higher turbulent intensities significantly decreasing the reattachment length. According to Hunt, flow probably reattaches, unless building length is small compared to the width and height. If flow reattachment does not occur, the flow at the side and top of the building form one big recirculation cell (also called separation cavity) with the flow behind the building. If flow reattachment occurs, a separate recirculation cell is formed behind the downwind edges of the building. Within the recirculation cell, two standing vortices occur at the building corners, forming an arch behind the building (Peterka et al., 1985; Martinuzzi & Tropea, 1993).

The recirculation cell is bounded by the streamline that reattaches to the ground surface (Fackrell, 1984; Peterka et al., 1985). As such, wind following streamlines under this elevation transport air into the recirculation cell. So by conservation of mass transport, air is also flowing out of the recirculation cell. This involves flow from the two standing vortices that is entrained in the larger horseshoe vortex. Furthermore, gusts of wind and turbulence can wash out the entire recirculation cell (Peterka et al., 1985). The vortices behind the building and the separation cell become more asymmetrical as relative building height increases, increasing cross-stream flows and turbulence (Wang & Zhou, 2009).

Downstream of the recirculation cell, the building wake still differs from the undisturbed airflow (Hunt, 1971; Peterka et al., 1985). In general, the mean velocity is lower. However, the turbulence is higher and vorticity is increased, especially in the tails of the horseshoe vortex. It takes some distance before the wind recovers. According to Peterka et al. (1985), the extent of the wake is 10 to 30 building heights for buildings with a width of 1 to 4 times their height. The velocity deficit in the building wake decays with $x^{-1.5}$ behind a cubical building (Hunt, 1971; Peterka et al., 1985) and with x^{-1} behind a low (and perpendicular to the wind) long building (Hunt, 1971). In addition, the results of Peterka et al. (1985) seem to indicate that for high narrow buildings, the velocity deficit also decays with x^{-1}. With regards to the turbulent intensity excess, wind tunnel experiments from Peterka indicate that it decays with x^{-2}, so faster than the velocity deficit. However, according to calculations and field measurements of Hunt (1971), the turbulent intensity excess decays slower than the velocity deficit.

Within the building wake, the velocity deficit (flow deceleration) is strongest on the centreline behind the building (Peterka et al., 1985). About 0.5 to 0.75 building widths from the centreline, the velocity deficit is lower, as the downward flow of the horseshoe vortex convects stronger winds from higher elevations down. At approximately 1 to 1.5 building widths from the centreline, the velocity deficit increases again, as the upwards flow in the horseshoe vortex convects slower winds up (see Peterka et al., 1985, fig. 8).

The upwind separation length (L_F) and the size of the vortex in front of the building depend on the building height and width (Beranek, 1984; Peterka et al., 1985; Martinuzzi & Tropea, 1993) and on the turbulence intensity (Peterka et al., 1985). Martinuzzi and Tropea (1993) found that the upwind separation length initially increases with the building width, to subsequently become relatively constant. (Using W, H and L for the building width, height and length, L_F increased from $0.7H$ for buildings with an aspect ratio (W/H) of 1 to $1.4H$ for an aspect ratio of 6 or more (see Martinuzzi & Tropea, 1993, fig. 14)). Beranek (1984) found an upstream separation length of $0.7\sqrt{WH}$ for aspect ratios between 0.8 and 3.

Martinuzzi and Tropea (1993) note that the initial increase of the separation length (with building width) implies that for buildings with a smaller aspect ratio, the flow is mostly deflected to the sides. In this case, the amount of deflected flow increases proportionally with the building width. Consequently, the separation cell grows and the separation length increases. For larger aspect ratios, the wind is increasingly deflected over the building. Hence, the separation length becomes almost constant. This transition coincides with a changing flow structure: for building width larger than 10H, multiple nodes and saddle points occur, forming a row of adjoining horseshoe vortices (see Martinuzzi & Tropea, 1993, fig. 5).

The separation length at the rear of the building (L_R) depends on the building height (Wilson, 1979; Beranek, 1984; Fackrell, 1984; Peterka et al., 1985; Martinuzzi & Tropea, 1993), building width (Wilson, 1979; Beranek, 1984; Fackrell, 1984; Martinuzzi & Tropea, 1993), building length (Fackrell, 1984) and on the turbulent intensity (Fackrell, 1984). When defined as the length between the rear of the building and the centreline reattachment point downwind of the building, L_R can vary between 2 and 6 building heights according to Peterka et al. (1985). Wilson (1979) found L_R to be equal to what he defined as the building scaling length R (eq. 3.1). Martinuzzi and Tropea (1993) found that L_R scales approximately linear with the rescaled building width up to $L_R \approx 4H$ for $W/H=4$, to then asymptotically reach a maximum value of about 7.2H. In comparison to the upstream separation lengths they found, the downstream separation lengths were more than twice as long. Using multiple field and wind tunnel experiments, Fackrell (1984) developed eq. 3.4, to express how L_R increases with building width and height, but decreases with building length (adapted from Hosker, as cited by Fackrell). In this equation, L/H should range between 0.3 and 3, if not the nearer limit should be used. Hosker (as cited by Fackrell) further quantified how L_R increases if the boundary layer on top of a building does not reattache before the end of the building. Additionally, Fackrell noted that in wind tunnel experiments L_R decreases slightly with increasing turbulence, but is mostly independent of the wind speed. For a cubic building of size 1, the results for L_R according to the different expressions is indicated in Figure 11.

$$R = B_S^{0.67} \cdot B_L^{0.33} \qquad (3.1)$$

with

$$B_S = \min(W, H) \qquad (3.2)$$

$$B_L = \max(W, H), \quad B_L \leq 8B_S \qquad (3.3)$$

$$L_R = \frac{1.8W}{(L/H)^{0.3} * (1 + 0.24\,W/H)} \tag{3.4}$$

Schulman et al. (2000) also described the lateral width of the separation cavity and building wake. This is shown in eq. 3.5 to 3.7, with W_C resp. W_W the width of the cavity and the building wake (measured from the centre line and with x starting at the front of the building) and R the building length scale. Using a cubic building of size 1, this results in a circulation cavity as sketched in Figure 11.

$$W_C = \frac{W}{2} + \frac{R}{3} - \frac{(x-R)^2}{3R}, \qquad 0 < x < R, \tag{3.5}$$

$$W_C = \left(\frac{W}{2} + \frac{R}{3}\right)\sqrt{1 - \left(\frac{x-R}{L + L_R - R}\right)^2}, \qquad R < x < L + L_R \tag{3.6}$$

$$W_w = \frac{W}{2} + \frac{R}{3}\left(\frac{x}{R}\right)^{1/3} \tag{3.7}$$

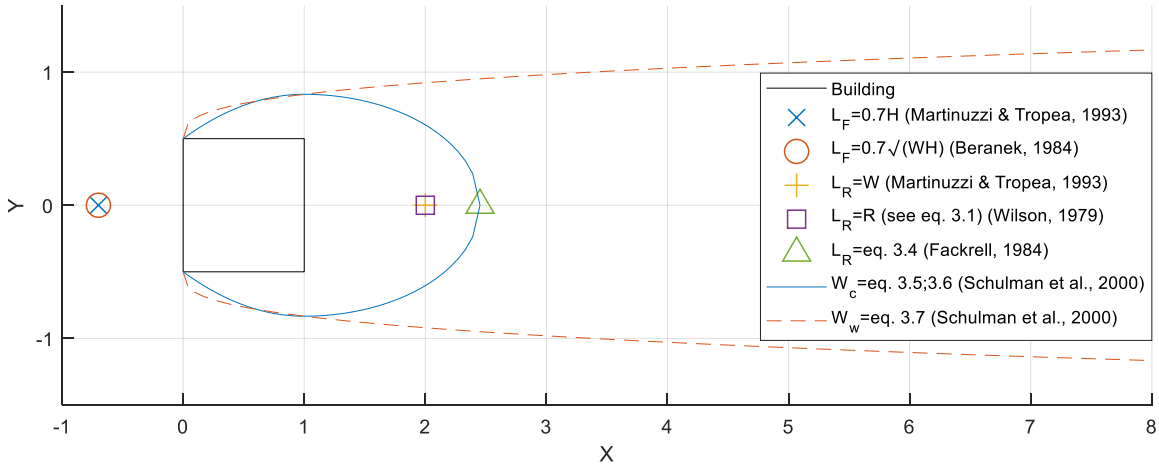

Figure 11: Flow separation locations around a cubical building according to literature: upstream separation length (L_F), downstream separation length (L_R), cavity width (W_C) and wake width (W_W). Eq. 3.4 and the downwind length of the cavity according to Schulman et al. (2000) coincide by definition. The other coincidences of L_F and L_R are because only occur when building width and height are equal. NB: The factor 0.7 in $L_F = 0.7H$ depends on the W/H ratio.

In these expressions, the building wake width continuously increases in size. However, Martinuzzi and Tropea (1993) found that the width of the cube wake decreases up to (approximately) the reattachment point, after which the distance increases again. Martinuzzi and Tropea (1993) think the narrowing is caused by recirculation vortex initially entraining fluid towards the centre axis. Behind the recirculation cell, the average flow in the reattached wake is away from the centreline (while the flow outside of the wake is by definition in the streamwise direction). The expansion of the wake is caused by entrainment of outward flow into the horseshoe vortex. This narrowing and widening of the wake is also visible in the results of Peterka et al. (1985, fig. 1 and 8).

The description above applies to cubic shapes oriented perpendicular to the flow. Depending on building design and orientation, other flow structures can occur as well. Especially for buildings oriented at an angle to the flow, a pair of rooftop vortices originates from the front edges (Castro & Robins, 1977; Peterka et al., 1985). If one of these vortices is stronger than the

other, this can dramatically extend the length of the wake. Peterka et al. (1985) found that for a building at a 45-degree angle, the velocity deficit in the wake was still apparent after 80 building heights, while it would normally be negligible after 10 to 30 building heights. However, Castro and Robins (1977) found that the strong rooftop vortices decay quite quickly, such that the velocity components after 6 building lengths are very similar to the velocities behind a cube normal to the flow. For the reattachment length behind the building (L_R), Fackrell (1984) found that a building orientation diagonal to the wind leads to values that are about 20 per cent larger.

3.2 MORPHOLOGICAL EFFECTS FROM BUILDING PRESENCE

3.2.1 THE BEACH AND DUNES: SCIENTIFIC LITERATURE

As a result of the changes in wind flow around buildings, the reduction in the source area and the direct blockage of sediment transport, buildings affect the sediment transport and beach-dune morphology in their surroundings. Effects of buildings on top of dunes and at the landward side of dunes were studied by Nordstrom et al. on Fire Island and Westhampton Beach, two barrier islands near New York (Nordstrom & McCluskey, 1984: Fire Island; Nordstrom & James, 1985: Fire Island; Nordstrom et al., 1986: Westhampton Beach).

On Westhampton Beach, Nordstrom et al. (1986) observed that the seaward side of the dunes was approximately linear, while the landward side had a crenulated barchanoid shape. This resulted from the combination of the changed wind field and landscaping efforts by building owners. Offshore winds were accelerated as they blew around the house and caused scour behind the house. Residents erected bulkheads and pushed sand of their property to keep their terraces and patios free of sand. In general, they preferred to push the sand to the sides of the property, rather than towards the crest of the dune (where it would again be blown on the property). Hereby they increased the size of the horns of the dune and reinforced the crenulated shape. This shape in turn contributed to the convergence of the flow and hence the scour behind the house.

On fire Island, a barrier island adjacent to Westhampton Beach, Nordstrom and McCluskey (1984, 1985) studied isolated houses built on top of and landward of the dunes, paying special attention to the effect of building on pilings. They found reduced wind speeds in the lee of a building, also for elevated buildings. This promoted deposition. Houses built on pilings showed a scour zone of approximately 0.5 m below the undisturbed ground surface, caused by increased wind velocities and a lack of vegetation (see Figure 12). Around the houses deposition increased, leading to a lip of approximately 0.5 metres above the undisturbed surface. Houses built behind the dune crest at a lower elevation had a larger effect than houses built on top of the dune. During the landward dune migration that occurred, high wind speeds under the house prevented sedimentation and burial of the house, thereby causing a depression in the area surrounding the house. Houses built directly on the ground, including elevated buildings with temporary breakaway walls to the ground, were more complete sediment traps. For houses with breakaway walls, they observed sedimentation deposits reaching the first floor of the house.

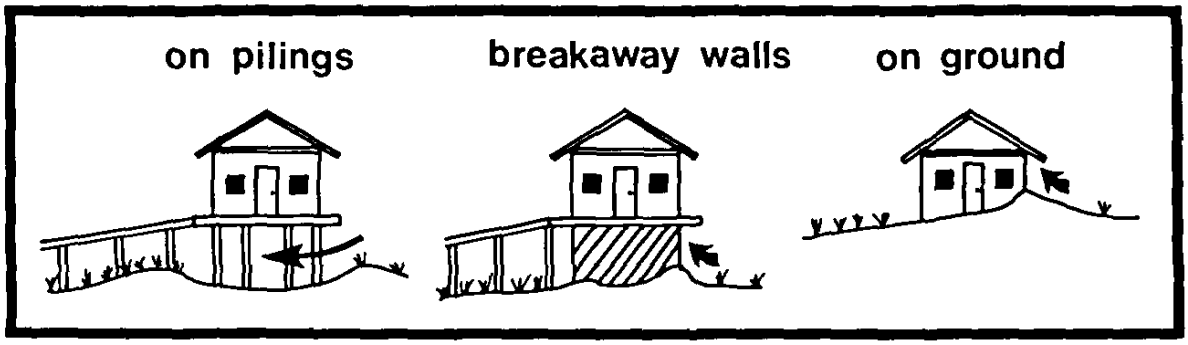

Figure 12: A schematic representation of different types of houses, their airflow and the resulting morphology (figure 3 Nordstrom & McCluskey, 1984)

High rise buildings have due to their size a larger effect on wind patterns and speeds and affect a wider area than normal houses (Jackson & Nordstrom, 2011). Nordstrom and Jackson (1998) used scale experiments and field observations to study the effects of an 80 metres high hotel in Atlantic City, New Jersey. In agreement with other literature (see also previous section), they found high wind speeds around the building, and flow separation and upwards wind flows, especially in the lee. As a result of the flow reversal and high wind speeds, sand from the beach was blown to the boardwalk and hotel during offshore wind conditions. Furthermore, the sand transport layer was more than 2 metres high, and at times a sand cloud was visible 10 metres above the boardwalk, compared to 0.5 metres above the beach. At the backshore, highly local scour and deposition zones were created.

Houses built on the beach in front of a dune can be compared to natural vertical cliffs found in deserts and at beaches (Tsoar, 1983; Tsoar & Blumberg, 1991). Tsoar (1983) used a wind tunnel to examine the echo dune formation upwind of cliffs. Echo dunes are single sand riches that form a small distance upwind of vertical cliffs. Using upwind distance d and cliff height h, he observed an initial separation distance between the cliff and dune was at d/h is 0.3 to 0.4, while the crest of the dune was located at an upwind distance of d/h is 0.5 to 0.6. As the echo dune grew higher, the crest remained at the same location, but the edge of the dune moved closer to the cliff (see Tsoar, 1983, Fig. 5). Furthermore, he noted that similar echo dunes can be found at buildings in front of buildings in a desert.

The effect of adjacent cities is examined in a number of studies on the effect of urbanization at the Canary Island on adjacent dune fields (Malvarez et al., 2013; Hernández-Calvento et al., 2014; García Romero et al., 2016; Smith et al., 2017b). Buildings replaced the source areas for dunes and cut dune fields of from their sediment sources (Malvarez et al., 2013; Smith et al., 2017b). Hernández-Calvento et al. (2014) and Smith et al. (2017b) studied the effect of increasing urbanization at Maspalomas on the adjacent dune field using CFD modelling. They found profound changes to the wind field, turbulent intensity, and flux potential. Hernández-Calvento et al. (2014) found wind speed deceleration of up to 50 per cent in the shadow zone behind the urbanization and acceleration of 30 per cent at the southern tip of the urbanization. According to Smith et al. (2017b), the flux potential in these zones decreased resp. increased by 80 per cent. Furthermore, they found flow deflections (changes in wind direction) up to 20 degrees (Hernández-Calvento et al., 2014) and 25 degrees (Smith et al., 2017b). In addition, Smith et al. (2017b) noted an increased turbulent intensity in the wake of the buildings. Furthermore, vegetation cover increased both in the urban shadow zone and the deflation

areas in the acceleration zone (Smith et al., 2017b). Near the beach, human influences caused a decrease in vegetation cover (Hernández-Calvento et al., 2014).

As a result of these changes, flow at the dune length scale is modified, with changes to the stoss-side and lee-side flow of dunes and secondary airflow dynamics (turbulent vortices shaping the dunes) (see Smith et al., 2017b). At the larger dune field scale, dune dynamics and erosion decreased in the urban shadow zone (Smith et al., 2017b). In the acceleration zone south of the urban developments, erosion rates and deflation area presence increased and dune migration accelerated (Smith et al., 2017b). This in turn resulted in the coalescence of landward migrating smaller dunes near the coast and the formation of a migrating accumulation ridge (Hernández-Calvento et al., 2014; Smith et al., 2017b). As a result, the area near the coast here shows a sediment deficit and a net decrease in elevation.

3.2.2 THE BEACH AND DUNES: PROFESSIONAL LITERATURE

In professional literature, predominantly written for water managers and regional authorities, more case studies and quantitative effects can be found. Hoonhout and Van Thiel de Vries (2013) from Deltares examined existing literature and data sets on the effect of buildings on Dutch beaches. Hereto they used 1D cross-shore profiles ("Jarkus raaien") of the Dutch coast and a Bayesian network[1] to determine if the presence of buildings on beach significantly affects the magnitude and trend of the dune volume. They could not find a significant effect on dune volume, but concluded that buildings have a significant negative effect on the dune volume trend. Continuous structures, such as rows of holiday homes, had an especially strong effect; stronger than a few separate large constructions. However, it was sometimes unclear whether the effect from the mere presence of buildings was measured, or of the usage of buildings. Based on their findings, they advised to 1) keep a minimum distance of 1 building width between buildings, with special care for year-round occupation; 2) keep a minimum distance of 5 metres between a building and the toe of the dune and 3) make rules for and check on the effects the usage of buildings (predominantly removal of sediment deposits by building owners).

Furthermore, Hoonhout and Van Thiel de Vries (2013) made some more concrete observations for the building shape and type. Buildings that were only present during summer still showed a negative effect on trends in dune volume. A study by Van der Valk and Van der Meulen (2013) on the effect of beach houses near Spanjaardsduin supported these findings: these houses there were only present in summer, but still showed increased sedimentation at the seaward side and decreased sedimentation and less dense vegetation directly behind the house. Looking at the duration of the summer occupation, Hoonhout & Van Tiel could find no effect (on the dune volume trend). To spatially examine the morphological changes around different buildings, they used lidar maps of the elevation around buildings. They observed decreased sedimentation or even erosion of the beach and dune directly behind continuous buildings. For separate beach pavilions, they observed sedimentation in front of the buildings and erosion behind them. Near Katwijk aan Zee they discovered erosion at the beach in front of the houses

[1] Bayesian networks are probabilistic graphical models, in which the graphical structures represent relations (probabilistic dependencies) between variables. They are suitable to calculate the conditional probabilities (Ben-Gal, 2009), here e.g. the probability of a negative trend in dune volume, given the presence of a building on the beach.

and increased bed levels around the buildings, indicating that sand from the beach was used to (actively) increase the elevation near the buildings.

Van Beeck et al. (2011) used scale models in a wind tunnel to examine the effect of continuous rows of buildings on Spanjaardsduin. In a general sense, their results confirm the significant effect that buildings have in their direct surroundings. More specifically, they concluded that the wind at the ground level is decelerated around houses, promoting deposition and local dune formation. Simultaneously, this deposition implies a decreased sand transport to the hinterlying dune. The increased deposition leads to the formation of a slope in front of the building. Once this slope reaches its equilibrium height, grains use it to jump over both the house and the low-velocity area behind it, thereby explaining the lack of sedimentation directly behind the houses in the experiment. Scaled back to the real (full-size) timescale, this built-up of the slope took 9 days.

Hoonhout and Van Thiel de Vries (2013) also placed their findings in perspective. Other factors than the buildings, such as nourishments, had a far stronger effect on the trend in dune volume. And the expected increase of the hydrodynamic erosion caused by a normative storm is often an order of magnitude smaller than the average increase in dune volume along the Dutch coast. So if this trend continues, dunes will generally remain safe under sea-level rise. Only locally a critical situation could occur. This would depend more on nourishments than on the effects of buildings. Consequently, they saw no reason to advise against buildings on the beach in general, if care is taken to minimize the negative effects of buildings on duneward sediment transport.

In a follow-up report in 2014, Hoonhout and Waagmeester (2014) tried to determine the effect of more variables (building size, distance between buildings, placement period) by including them in the Bayesian network. This was not possible, as the variation in the data was insufficient to quantitatively asses the effect of the different building properties on the dune volume trend with the Bayesian network (i.e. combinations of properties were missing, and some properties were correlated). This matched the results of Huisman (2013), who examined the monitoring plan and monitoring data of HHNK (a regional water authority in the Netherlands). He found that within his data set, negative trends in dune volume occurred behind buildings but not in reference areas. However, due to the limited dataset, no conclusions could be drawn on the significance of these results and the effect of different building properties.

Reinders et al. (2014) from Deltares used a different approach, using Google Earth images to examine the effect of various types of buildings built in front of a dune on the dune dynamics of Spanjaardsduin. They concluded that buildings have a negative effect on dune dynamics (i.e. patchiness and variation in dune shape and vegetation cover). This effect becomes stronger as the distance between buildings decreases and building size increases. Small solitary houses had slight erosion directly behind the houses and barely any effect on the width of the dynamic zone of the dune. Rows of houses with gaps decreased the dynamic zone width. In addition, in one case the dynamic zone was partly replaced by a bare sedimentation area. Continuous rows of houses decreased the width of the dynamic dune zone further. Large beach pavilions also showed a significant effect, with erosion to the side and at the back corners and sedimentation directly behind pavilions. To prevent the buildings from becoming a barrier to sand transport, they advised limiting the maximum continuous length of beach houses (to 25 m, with gaps of at least 15 m in between). In addition, they advised to keep some distance between buildings – buildings here including terraces with wind screens – and the dune.

De Zeeuw (2017) continued the analysis of effects around buildings using aerial images, using camera-equipped UAVs instead of Google Earth. This increased the temporal resolution (multiple flights in 2015-2016 at two locations along the Dutch coast) and the spatial resolution. In addition, it allowed for the use of photogrammetry to build DEMs (digital elevation maps) and determine elevation changes in unvegetated areas. In general, they observed erosion directly around buildings, while a deposition zone often occurred at some distance downwind of the buildings. They further observed significant differences in the deposition volume in the dune zone behind buildings: on average 7.2 m^3/m in one year in the reference zones without buildings versus 1.2 m^3/m behind the buildings. Focusing on different building types, the zone behind beach pavilions showed barely any development, while some deposition could be found behind rows of houses (on average -0.1 m^3/m resp. +1.5 ^{3}/m in a year, with the rows consisting of holiday houses with small gaps in between.

To further explore the effect of different building properties, Van Onselen (2018) used computational fluid dynamics (CFD) to model the airflow around buildings. He examined the effect of three measures to promote sediment transport to the dunes: 1) Building elevated on piles to allow wind flow and possible sediment transport underneath; 2) increasing the distance from the dune to decrease the possible effect on the dune and 3) increasing the distance between buildings, to allow for flow acceleration and possible sediment transport in between buildings. He found placing buildings on poles to be the most efficient solution to decrease their negative effects, with an advised pole height of 1.5 metres.

3.2.3 SNOW ACCUMULATION AROUND BUILDINGS

3.2.3.1 A SINGLE CUBE/BUILDING

The literature on snowdrift and accumulation around buildings provides further information on the sedimentation and erosion around buildings. Thiis and Gjessing (1999) examined snowdrifts around a cube with sides of 2.5 m and observed a deposition horseshoe that was interrupted at the upwind corners. Following the nomenclature as defined in Figure 13, the distance to the upwind deposition horseshoe was about 1.6 m, with a steep slope to a maximum height of about 80 cm and a gentle inclination at the windward slope of this deposition area. This agrees well with the upstream separation lengths as reported in other research: the estimates of $0.7H$ (Martinuzzi & Tropea, 1993) and $0.7\sqrt{WH}$ (Beranek, 1984) both result in a theoretical separation length of 1.75m.

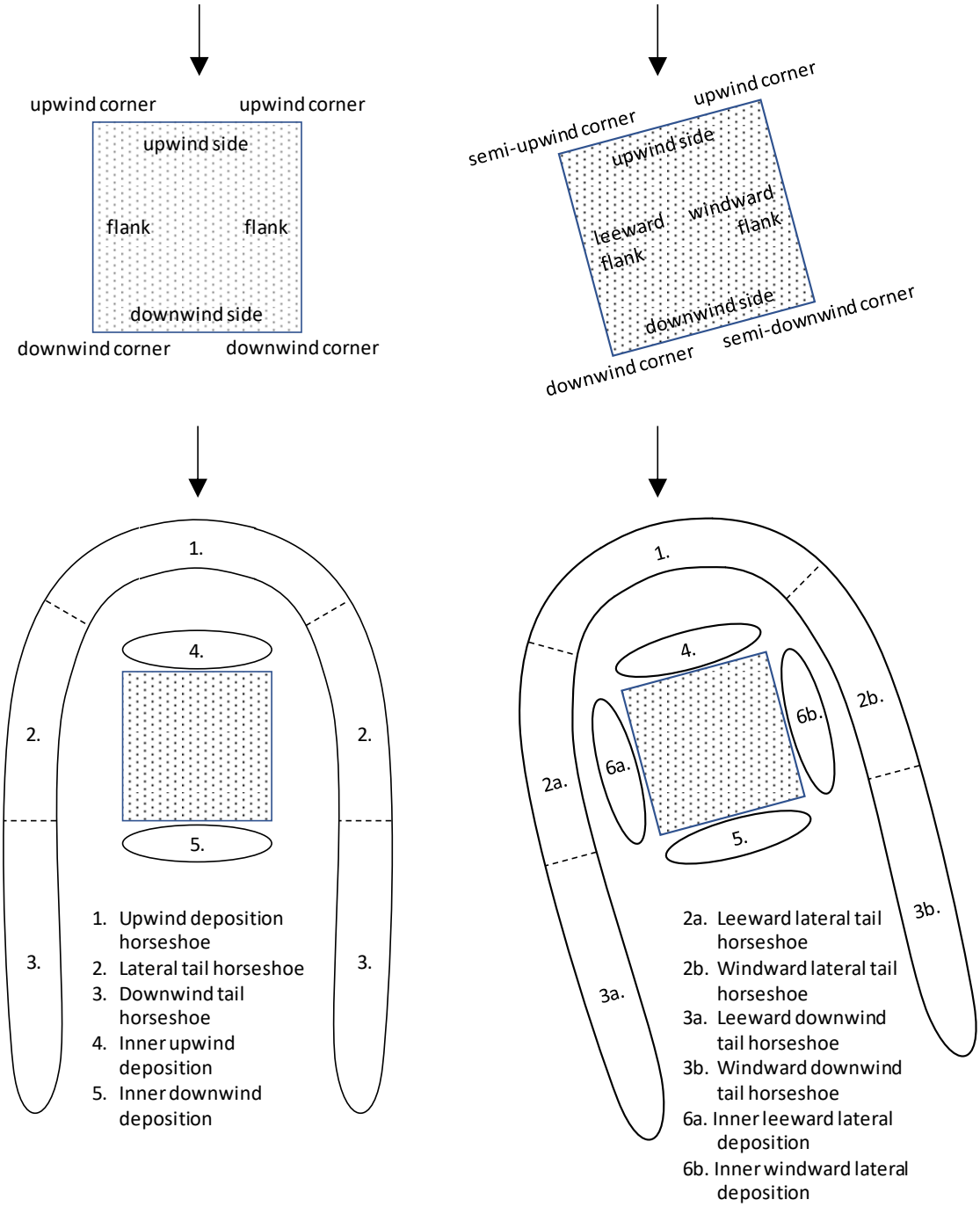

Figure 13: The locations and possible deposition features around a cube or building. A) The names used in this document for the corners and sides of a building facing a perpendicular wind. B) The names used for a building facing an oblique wind. C) The possible deposition features around a building facing a perpendicular wind. D) The possible deposition features for a building facing an oblique wind (names for features 1, 4 and 5 remain unchanged).

The horseshoe tails around Thiis and Gjessing's cube (1999) differed in size due to the oblique wind angle and varying wind direction, with the leeward deposition tail extending 30 m behind the building and the windward deposition tail extending 50 m behind the building. The shape of the tail followed the described horseshoe vortex, with a decreasing width until the, according to Thiis and Gjessing, centre reattachment point and an increasing width after this point. However, the point where the width increased was about twice as far as the expected

downwind reattachment distance from Martinuzzi and Tropea (1993) and Fackrell (1984), so possibly this transition to widening tails occurred downstream of the reattachment point.

The largest accumulation depth (80 cm) occurred just downward of this point, so where the wake expands and the mass flux increases. Within the horseshoe, no deposition areas were observed. The lack of an inner downwind deposition was explained by the transport mode in the experiment. Wind below the stagnation zone (2/3 to ¾ of the building height) flows to the sides and follows the horseshoe vortex, while wind above the stagnation zone can also blow over the building and be recirculated at the back. Hence only snow that is present higher in the air (i.e. snow that is in suspension) is expected to blow over the building and form an inner downwind accumulation ridge. The moderate wind speeds of the experiment apparently caused little suspensive transport.

3.2.3.2 WIND SPEED

Thiis (2003) also looked at the deposition behind a building-sized rectangular model of 2.5x7.5x2.5m. Starting with a flat bed, the development after 6 and 12 days was measured, with the first period having moderate winds (10 m/s, causing saltation) and the second period also having strong wind (15 m/s, causing suspension). The wind was approximately perpendicular to the long side of the building. Again clear upwind deposition and the downwind deposition tails were visible, while the lateral deposition tails were barely present. The distance to the upwind deposition horseshoe was approximately 2 m. This is significantly smaller than theoretical estimates for the upstream separation length: $1.2H$ from Martinuzzi and Tropea (1993) and $0.7\sqrt{WH}$ Beranek (1984) both result in 3 m.

Between the first and the second measurement, the upwind deposition area and downwind deposition tails grew slightly in size and height. The lateral deposition tails also became slightly more visible. The biggest change was in the inner downwind deposition area: this was barely visible after the first phase, but clearly visible in the end, thereby supporting the theory that suspensive transport is needed for this area to form. Within the downwind inner deposition area, deposition seemed strongest in the corners – so approximately at the location of the downwind corner arch vortex in Figure 10. Both the deposition horseshoe and inner downwind deposition showed similar development in a different set-up with two adjacent cubes.

Liu et al. (2018) examined the effect of the wind speeds up to 4.5 m/s on snow accumulation around a 0.5 m. large cube in a wind tunnel. This wind tunnel also contained a snowfall generator, thereby combining effects from snowfall and snowdrift. Upwind of the cube, they observed a single accumulation area touching the cube for low wind speeds (1.5-2.5 m/s) (see fig. 10 in Liu et al., 2018). This area extended to the sides and then in tails to the back, forming a horseshoe shape. For wind speeds of 3.5 and 4.5 m/s, there was some snow deposition directly against the cube, then a small distance without snow, and further upwind a larger accumulation area. For the 3.5 m/s this area extended to the side and back, forming the horseshoe shape. For the highest wind speed, no deposition occurred to the sides of the building, so the downwind deposition tails formed distinct accumulation areas. In addition, they observed some snow deposition directly behind the cube: a minimal amount for the lowest wind speeds and slightly increasing for higher wind speeds. For cubes angled to the wind, the inner downwind deposition areas only occurred for higher wind speeds.

Oikawa and Tomabechi (2000) also examined the effect of wind speed on the snowdrift, using a single cube with sides of 1.0 m and 7 repetitions at different natural wind conditions (1.5 to 5 m/s, so all too weak to cause suspension). The pattern they found was less clear, more resembling a reverse doughnut than a horseshoe shape, so with deposition mainly directly around the cube and in the area far away, with erosion in between. In general, the patterns they found became especially clear for wind speeds larger than the threshold friction velocity. Measured at the centreline, upwind deposition occurred up to ⅙L from the front of the building (the inner upwind deposition) and further than 1L from the building (probably the upwind deposition 'horseshoe'). The area in between experienced erosion. Below the threshold velocity, upwind sedimentation increased with wind speed. Above the threshold velocity, the upwind horseshoe deposition depth decreased with u. Downwind of the cube a similar pattern was visible. Deposition or light erosion occurred directly downwind of the cube: up to a distance of ⅙L to L from the cube, with larger distances for stronger winds. Erosion occurred from this point to 2 building lengths from the cube (at the centreline), followed again by snow accumulation. The erosion depth increased with wind speed. For the deposition to the sides of the cube, it varied per run whether this also occurred directly to the sides of the cube (inner lateral deposition), or only in the far field (the lateral horseshoe tails).

Comparing the results, Thiis (2003) showed that larger wind speeds promote the formation of an inner downwind deposition area. For Liu et al. (2018) this was already present at the lowest wind speeds - probably because of the presence of snowfall and possibly aided by the smaller model size – and increasing at higher wind speeds. Oikawa and Tomabechi (2000) observed some inner downwind deposition at lower wind speeds and an increasing length with increasing wind speeds. For the upwind deposition, Liu et al. observed that it was connected to the building for the lowest wind speeds, and that separation (and thereby an inner upwind deposition area) only appeared for wind speeds higher than 2.5 m/s. Oikawa and Tomabechi did not observe the really continuous upwind sedimentation of Liu et al., but did find that the erosion depth (between the inner upwind deposition and the upwind deposition horseshoe) increased with wind speed. The difference here might be due to the snowfall included in the experiments of Liu et al. Above the critical wind velocity, the upwind deposition horseshoe depth of Oikawa and Tomabechi also decreased with wind speed.

3.2.3.3 Building orientation

Liu et al. (2018) looked at the effect of building orientation. Using the same wind tunnel and scale model (a cube with sides of 0.5 m), they varied the angle of incidence between 0 and 45 degrees for wind speeds of 2.5 and 4.5 m/s. At low wind speed, the incidence angle of 10 degrees created a horseshoe that was very similar to the perpendicular case: a complete horseshoe that is connected to the cube at the upwind side and no downwind inner deposition. This horseshoe formed in the direction of the cube, so slightly slanted to the wind. For an incidence angle of 30 degrees, the horseshoe at the windward lateral side connected directly to the cube. The deposition depth at the upwind side remained higher than at the windward lateral side. The downwind tail at the leeward side is of a smaller volume and length than at the windward side (1 vs 2 building lengths). The incidence angle of 45 degrees created a symmetric pattern – more resembling an arrowhead than a horseshoe – with narrow sedimentation tails, a larger distance between the tails and some small inner downwind sedimentation.

For the larger wind speed of Liu et al. (2018), the wind angle of 10° again showed a slanted horseshow (with respect to the wind). The upwind deposition horseshoe and inner upwind deposition started to become distinct areas (i.e. two clearly separated maxima occurred with light deposition in between, so the complete separation that occurred with perpendicular winds was still lacking). Furthermore, the horseshoe was interrupted, with no leeward lateral deposition tail. The windward downwind deposition tail extended further and had a larger depth than the leeward tail. At an angle of 30°, the lateral windward tail again connected to the cube's side (like at 2.5 m/s), but without a distinction between the inner lateral deposition and the lateral tail (as visible for a perpendicular wind). The windward tail again was larger in area and depth, but of similar length as the leeward tail. A wind angle of 45° again created an arrow-head-like shape, with the upwind 'horseshoe' and inner upwind deposition starting to become distinct areas. The inner downwind deposition areas were clearly visible.

3.2.3.4 Set-ups with multiple buildings

Thiis and Jaedicke (2000) examined the effect of the distance between objects, using two cubes of 2.5 metres, with distances of 1.7, 4.8 and 5.9 metres in between. For the smallest distance, snow accumulated in one large horseshoe around the cubes. The upwind snowdrift horseshoe height was continuous (no local minimum in the centre between the cubes) and downwind centre snowdrift (so the location where the tail of the separate cubes would be) was lacking. This indicates that the objects acted as one big obstacle, with little wind flow in between. Some small inner downwind deposition areas were visible directly behind the cubes. With 4.8 m. in between the cubes, the upwind deposition showed two distinct maxima in front of each cube. In between the buildings, no snow was deposited, but just downwind of the cubes a centre snowdrift appeared, higher than the lateral snowdrifts but of a shorter length. Together, this indicates an increased wind flow in between the buildings. For the largest inter-cube distance, the deposition pattern indicated the superposition of two horseshoe vortices, with a clear centre snowdrift. The centre snowdrift was considerably higher than the lateral snowdrifts, but of a shorter length. Furthermore, small inner downwind deposition areas were visible. Streamline plots from CFD modelling by Thiis and Jaedicke supported the general transition from a single large horseshoe vortex to two superimposed vortices and could reasonably predict the distance between the front of the cube and the upwind accumulation area. However, representation of the presence/absence of accumulation varied per case and the length of the accumulation tails was greatly overestimated.

3.2.3.5 Elevated buildings

Beyers and Waechter (2008) compared the deposition around buildings at ground level and elevated buildings, using field measurements around buildings and CFD modelling. They noted that the upwind deposition (the upwind part of the deposition horseshoe) is reduced due to enhanced scour by the airflow under elevated buildings. The snow that is located directly downwind of the building for on-grade buildings, is moved further downwind, as the underside of the building and area directly behind it are cleared by scour. In addition, the results show that the horseshoe around buildings weakens or disappears when buildings are elevated: both in the field and CFD models, the main downwind deposition occurred in line with the building, instead on in the sedimentation tails to the side of the building.

3.2.3.6 ROOF DESIGN

Thiis and Gjessing (1999) briefly examined the effect of different roof designs, by comparing snow deposition around a flat cube with 2.5 m sides (also see section 3.2.3.1) to similarly-sized cubes with a single pitch roof, i.e. a sloping in either windward or leeward direction. The lateral horseshoe deposition was mostly continuous for the flat-roofed cube, somewhat interrupted for the sloped roof with the high wall facing downwind and clearly interrupted for the sloped roof with the high wall upwind. Also, for the pitched roofs, the downwind tails were of a shorter length than for the flat roof.

3.3 MORPHOLOGICAL EFFECTS FROM BUILDING USAGE

The previous section described how the *physical presence* of buildings at the beach affects beach-dune morphology. However, *building usage* introduces additional effects. Building users actively shape their surroundings, e.g. by removing sand from roads. Also, building usage and recreation in general unintentionally disturb the environment, e.g. by walking and driving on the beach. In this section, these effects of building usage and recreation in general are examined.

3.3.1 REDISTRIBUTING AND STEERING DEPOSITION

An important impact of building usage is the deliberate redistribution of (storm) deposits (Nordstrom, 2000; Jackson & Nordstrom, 2011). Sand is constantly being blown around at beaches, and a part of this sand deposits on roads, parking lots, terraces etc. Especially during storms these windblown deposits can be substantial. Also, storms that cause overwash can create additional hydrodynamic deposits within dunes and landward of the dunes. Deposits that form a nuisance to building owners and beachgoers are often removed. (Re)moving these deposits locally changes sediment volume and composition (Jackson & Nordstrom, 2011). Depending on where sediment is moved to (see also Figure 14), the sediment balance of the beach system and the dunes can also change. For buildings in front of dunes, sediment can be moved further seaward on the beach; to the dunes behind the houses; or to the sides. For houses and roads in the dunes, the sand can be pushed to the sides of roads, be dumped in the dunes, or be transported back to the beach by trucks. In all cases, unvegetated heaps of sand are formed, which can in turn be displaced by the wind again (Nordstrom, 2000). Alternatively, the heaps can also be overgrown with vegetation and form hummocky ‘disposal dunes’ (Nordstrom & Arens, 1998), possibly aided by vegetative matter and nutrients present within (Williams & Feagin, 2010).

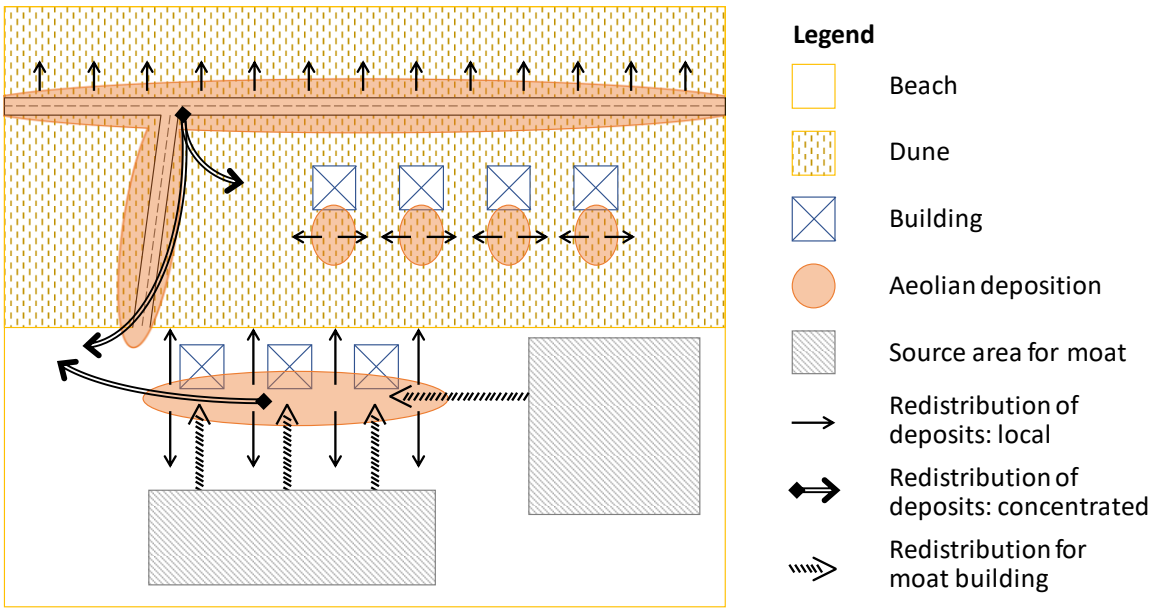

Figure 14: Typical types of human redistribution of sediment on the beach and in the dunes

Apart from reactively redistributing (storm) deposits, people also try to proactively steer deposition and change their surroundings. For instance, sand at the beach is bulldozered to form a local moat (Dutch: 'zandbanket'), so buildings can be placed at a saver elevation (Hoonhout & Van Thiel de Vries, 2013; Hoonhout & Waagmeester, 2014). Also, landowners build walls to prevent windblown deposition on their terrace or garden and steer where sand deposits (Nordstrom et al., 1986). Also, the gardens themselves change the dune dynamics (Jackson & Nordstrom, 2011). Artificial gardens around houses in the dunes differ in both surface roughness and vegetation type, density and height from natural dunes and are generally less mobile (Mitteager et al., 2006). Moreover, gardening can increase the nutrient content of the surrounding soil, thereby affecting the vegetation type and coverage in a larger area (Grunewald, 2006). Furthermore, removing unwanted sediment deposition from gardens can further change dune evolution. For instance, in a case study of Westhampton Beach, Nordstrom et al. (1986) found that backyards there were lower elevated than pathways between lots, due to residents shovelling unwanted deposition from their yard to the side.

3.3.2 WRACK REMOVAL

The removal of wrack (driftwood, seaweed or other vegetation and other stranded matter) to accommodate recreation is another human influence on beach-dune dynamics. On natural beaches, wrack provides a food source and habitat to beach fauna (Dugan et al., 2003; Dugan & Hubbard, 2010); creates a local topographic roughness that traps sediment and causes fetch segmentation (Dugan & Hubbard, 2010; Eamer & Walker, 2010; Jackson & Nordstrom, 2011); and contains nutrients and seeds and rhizomes of coastal vegetation that may germinate and grow into embryo dunes (Dugan et al., 2003; Cardona & García, 2008; Jackson & Nordstrom, 2011; Nordstrom et al., 2011). Hence, the removal of wrack, also called beach raking, decreases biodiversity and biodensity, generally increases sediment transport rates and suppresses the growth of embryo dunes, thereby increasing beach width. Dugan and Hubbard (2010) indeed found increased sediment rates at raked beaches: at least an order of magnitude higher. Conversely, Nordstrom et al. (2011), recorded lower transport rates on a raked beach than on a nearby unraked beach. Although they largely contributed this to differences in dune height, they also noted that especially fresh wrack has a significant effect; once covered by sand, the

effect is diminished. As advantageous use of removed wrack, Williams and Feagin (2010) demonstrated it can be used to fertilize dunes and stimulate dune growth. Combined, by increasing beach width and sediment transport, wrack removal causes (for onshore wind conditions) more sediment to be transported further onto the beach, to the first dunes or buildings. Of course, for offshore wind directions, seaward sediment transport is likewise increased (Jackson & Nordstrom, 2011).

3.3.3 WALKING AND DRIVING

Walking and driving at the beach or in dunes also affects beach-dune morphology, mainly by destroying vegetation and changing surface roughness. Trampling and destruction of wrack and vegetation (Rickard et al., 1994; Moffett et al., 1998; Houser et al., 2013), not only inherently has a range of ecological repercussions; it also diminishes the stabilization and trapping of sediment. This causes increased windblown sediment transport, inhibits dune formation at the beach and potentially creates blowouts in the dunes. Furthermore, driving changes the surface roughness, compacts the soil, and creates tracks (Jackson & Nordstrom, 2011; Witmer & Roelke, 2014). On the beach, long shore-parallel tracks can trap sediment and significantly decrease transport rates (Nordstrom et al., 2011). However, if recreational driving is restricted and only infrequent municipal patrols are allowed, these effects are probably limited (Jackson & Nordstrom, 2011). Moreover, walking and especially driving on a (sloping) beach also directly displaces sediment, on average in seaward direction (Anders & Leatherman, 1987; Schlacher & Thompson, 2008). For instance, Anders and Leatherman (1987) estimated that cars driving at the beach at Fire Island moved seaward up to 120.000 m^3 of sediment per year. In addition to these morphological effects, driving also has ecological effects, by e.g. destroying vegetation, crushing invertebrates (Schlacher et al., 2007), disturbing birds (McLeod et al., 2013; Weston et al., 2014) and creating tracks that act as barrier to hatching turtles (Aguilera et al., 2019).

3.3.4 BUILDING REMOVAL

Although all these factors show that the presence and usage of buildings can have a pronounced effect on beach-dune morphology, removing buildings from the dunes is also not without consequences. Removing buildings from the dunes leaves unvegetated patches behind. Of course, bare areas also occur under natural conditions, but Nordstrom and McCluskey (1984) found that on Fire Island, New York, many bare patches were created by the removal of houses. These patches recovered slowly, and frequently even grew in size, eventually becoming blowouts.

4

CONCLUSION

Buildings in the beach-dune system primarily affect the morphology in their surroundings, because they disturb the wind field and sediment transport (Hunt, 1971; Jackson & Nordstrom, 2011; Smith et al., 2017b). The wind flow around a single cuboid building is relatively well understood. There is ample research on the wind flow patterns around a single cuboid object, in the form of wind tunnels (Castro & Robins, 1977; Fackrell, 1984; Martinuzzi & Tropea, 1993), field studies (e.g. Hunt, 1971) and numerical simulations (Meroney et al., 1999; Schulman et al., 2000). These studies give a good overview of the flow patterns and quantitative predictions of where flow separation occurs. However, there is little research on the effect of more complicated building shapes than cubes and on interactions between (airflows over) buildings and dunes.

The airflow around buildings determines the effects on sediment transport and morphology. However, the steps from wind flow to wind-blown sediment transport to morphology (bed level change) are far from straightforward (Kok et al., 2012). The literature is clear that buildings on the beach or in the dunes have a pronounced effect on beach-dune morphology. Buildings are shown to cause patterns of deposition and erosion (Nordstrom & McCluskey, 1984; Van Beeck et al., 2011). Furthermore, they decrease the source area for sediment transport and cause fetch segmentation (Morton et al., 1994; Jackson & Nordstrom, 2011). Buildings, and especially people using buildings, also disturb vegetation, thereby further interfering with the natural beach- and dune-shaping processes (Mitteager et al., 2006; Houser et al., 2013). Moreover, people actively redistribute sand around buildings, mainly to keep buildings and roads usable when faced with unwanted (storm) deposits (Nordstrom et al., 1986; Jackson & Nordstrom, 2011). Combined, by these effects, buildings can change dune shape (Nordstrom et al., 1986) and negatively affect dune volume trends (Hoonhout & Van Thiel de Vries, 2013).

However, to really predict and mitigate these effects, the dependency of the effect on design parameters (e.g. number, density, size, shape and location of buildings) should be understood (Nordstrom & McCluskey, 1984; Hoonhout & Waagmeester, 2014). Unfortunately, existing research on morphological effects around buildings pays little attention to these design parameters, or at most examines them on a qualitative level (Nordstrom & McCluskey, 1984; Hoonhout & Van Thiel de Vries, 2013). More fundamental research on effects of building shape and size under various conditions is predominantly on snow deposition around buildings (see section 3.2.3), although initial CFD examinations on possible sand deposition also exist (Van Onselen, 2018). A knowledge gap remains on the systematic quantitative effect of building properties on local sediment deposition an erosion (Hoonhout & Waagmeester, 2014); the interaction of configurations with multiple buildings and the combined effect of buildings and dunes.

REFERENCES

Aguilera, M., Medina-Suárez, M., Pinós, J., Liria, A., López-Jurado, L. F., & Benejam, L. (2019). Assessing the effects of multiple off-road vehicle (ORVs) tyre ruts on seaward orientation of hatchling sea turtles: implications for conservation. *Journal of Coastal Conservation, 23*(1), 111-119. doi:10.1007/s11852-018-0641-x

Anders, F. J., & Leatherman, S. P. (1987). Disturbance of beach sediment by off-road vehicles. *Environmental Geology and Water Sciences, 9*(3), 183-189. doi:10.1007/bf02449950

Andersen, U. V. (1995). Resistance of Danish coastal vegetation types to human trampling. *Biological Conservation, 71*(3), 223-230. doi:10.1016/0006-3207(94)00031-K

Andreotti, B. (2004). A two-species model of aeolian sand transport. *Journal of Fluid Mechanics, 510*, 47-70. doi:10.1017/S0022112004009073

Andreotti, B., Claudin, P., & Pouliquen, O. (2010). Measurements of the aeolian sand transport saturation length. *Geomorphology, 123*(3-4), 343-348. doi:10.1016/j.geomorph.2010.08.002

Bagnold, R. A. (1937). The Transport of Sand by Wind. *The Geographical Journal, 89*(5), 409-438. doi:10.2307/1786411

Bagnold, R. A. (1941). *The Physics of Blown Sand and Desert Dunes*. Londen: Chapman & Hall.

Bauer, B. O., Davidson-Arnott, R. G. D., Hesp, P. A., Namikas, S. L., Ollerhead, J., & Walker, I. J. (2009). Aeolian sediment transport on a beach: Surface moisture, wind fetch, and mean transport. *Geomorphology, 105*(1), 106-116. doi:10.1016/j.geomorph.2008.02.016

Bauer, B. O., Houser, C. A., & Nickling, W. G. (2004). Analysis of velocity profile measurements from wind-tunnel experiments with saltation. *Geomorphology, 59*(1), 81-98. doi:10.1016/j.geomorph.2003.09.008

Ben-Gal, I. (2009). Bayesian Networks. In F. Ruggeri, R. S. Kenett, & F. W. Faltin (Eds.), *Encyclopedia of Statistics in Quality and Reliability*: John Wiley & Sons.

Beranek, W. (1984). Wind environment around single buildings of rectangular shape. *Heron, 29*(1), 4-31.

Beyers, M., & Waechter, B. (2008). Modeling transient snowdrift development around complex three-dimensional structures. *Journal of Wind Engineering and Industrial Aerodynamics, 96*(10-11), 1603-1615. doi:10.1016/j.jweia.2008.02.032

Blocken, B., Stathopoulos, T., Carmeliet, J., & Hensen, J. L. M. (2011). Application of computational fluid dynamics in building performance simulation for the outdoor environment: an overview. *Journal of Building Performance Simulation, 4*(2), 157-184. doi:10.1080/19401493.2010.513740

Cardona, L., & García, M. (2008). Beach-cast seagrass material fertilizes the foredune vegetation of Mediterranean coastal dunes. *Acta Oecologica, 34*(1), 97-103. doi:10.1016/j.actao.2008.04.003

Carter, R. W. G. (1991). Near-future sea level impacts on coastal dune landscapes. *Landscape Ecology, 6*(1), 29-39. doi:10.1007/bf00157742

Castro, I. P., & Robins, A. G. (1977). The flow around a surface-mounted cube in uniform and turbulent streams. *Journal of Fluid Mechanics, 79*(2), 307-335. doi:10.1017/S0022112077000172

Chepil, W. S. (1945a). Dynamics of Wind Erosion .1. Nature of Movement of Soil by Wind. *Soil Science, 60*(4), 305-320. doi:10.1097/00010694-194510000-00004

Chepil, W. S. (1945b). Dynamics of Wind Erosion .2. Initiation of Soil Movement. *Soil Science, 60*(5), 397-411. doi:10.1097/00010694-194511000-00005

Chepil, W. S. (1945c). Dynamics of Wind Erosion .3. The Transport Capacity of the Wind. *Soil Science, 60*(6), 475-480. doi:10.1097/00010694-194512000-00006

Claudin, P., & Andreotti, B. (2006). A scaling law for aeolian dunes on Mars, Venus, Earth, and for subaqueous ripples. *Earth and Planetary Science Letters, 252*(1-2), 30-44. doi:10.1016/j.epsl.2006.09.004

Davidson‐Arnott, R. G. D., Yang, Y., Ollerhead, J., Hesp Patrick, A., & Walker Ian, J. (2007). The effects of surface moisture on aeolian sediment transport threshold and mass flux on a beach. *Earth Surface Processes and Landforms, 33*(1), 55-74. doi:10.1002/esp.1527

De Winter, R. C., & Ruessink, B. G. (2017). Sensitivity analysis of climate change impacts on dune erosion: case study for the Dutch Holland coast. *Climatic Change, 141*(4), 685-701. doi:10.1007/s10584-017-1922-3

De Zeeuw, R. C. (2017). *Effecten strandbebouwing op strand- en duinontwikkeling*. Retrieved from Den Haag:

Delgado-Fernandez, I. (2010). A review of the application of the fetch effect to modelling sand supply to coastal foredunes. *Aeolian Research, 2*(2-3), 61-70. doi:10.1016/j.aeolia.2010.04.001

Dong, Z., Wang, H., Liu, X., Li, F., & Zhao, A. (2002). Velocity profile of a sand cloud blowing over a gravel surface. *Geomorphology, 45*(3), 277-289. doi:10.1016/S0169-555X(01)00159-3

Dong, Z., Wang, H., Liu, X., & Wang, X. (2004). The blown sand flux over a sandy surface: a wind tunnel investigation on the fetch effect. *Geomorphology, 57*(1), 117-127. doi:10.1016/S0169-555X(03)00087-4

Duarte-Campos, L., Wijnberg, K., & Hulscher, S. (2018). Estimating Annual Onshore Aeolian Sand Supply from the Intertidal Beach Using an Aggregated-Scale Transport Formula. *Journal of Marine Science and Engineering, 6*(4), 127.

Dugan, J. E., & Hubbard, D. M. (2010). Loss of coastal strand habitat in southern California: the role of beach grooming. *Estuaries and Coasts, 33*(1), 67-77. doi:10.1007/s12237-009-9239-8

Dugan, J. E., Hubbard, D. M., McCrary, M. D., & Pierson, M. O. (2003). The response of macrofauna communities and shorebirds to macrophyte wrack subsidies on exposed sandy beaches of southern California. *Estuarine, Coastal and Shelf Science, 58*, 25-40. doi:10.1016/S0272-7714(03)00045-3

Durán, O., Claudin, P., & Andreotti, B. (2011). On aeolian transport: Grain-scale interactions, dynamical mechanisms and scaling laws. *Aeolian Research, 3*(3), 243-270. doi:10.1016/j.aeolia.2011.07.006

Durán, O., & Herrmann, H. J. (2006). Vegetation Against Dune Mobility. *Physical Review Letters, 97*(18), 188001. doi:10.1103/PhysRevLett.97.188001

Eamer, J. B. R., & Walker, I. J. (2010). Quantifying sand storage capacity of large woody debris on beaches using LiDAR. *Geomorphology, 118*(1), 33-47. doi:10.1016/j.geomorph.2009.12.006

Fackrell, J. (1984). Parameters characterising dispersion in the near wake of buildings. *Journal of Wind Engineering and Industrial Aerodynamics, 16*(1), 97-118.

Feagin, R. A., Smith, W. K., Psuty, N. P., Young, D. R., Martínez, M. L., Carter, G. A., . . . Koske, R. E. (2010). Barrier Islands: Coupling Anthropogenic Stability with Ecological Sustainability. *Journal of Coastal Research*, 987-992. doi:10.2112/09-1185.1

Fernandez Luque, R., & Van Beek, R. (1976). Erosion And Transport Of Bed-Load Sediment. *Journal of Hydraulic Research, 14*(2), 127-144. doi:10.1080/00221687609499677

Fletcher, B. (1976). The incipient motion of granular materials. *Journal of Physics D: Applied Physics, 9*(17), 2471.

García Romero, L., Hernández-Cordero, A. I., Fernández-Cabrera, E., Peña-Alonso, C., Hernández-Calvento, L., & Pérez-Chacón, E. (2016). Urban-touristic impacts on the aeolian sedimentary systems of the Canary Islands: conflict between development and conservation. *Island Studies Journal, 11*(1), 91-112.

Gilbert, M., Pammenter, N., & Ripley, B. (2008). The growth responses of coastal dune species are determined by nutrient limitation and sand burial. *Oecologia, 156*(1), 169-178.

Grunewald, R. (2006). Assessment of Damages from Recreational Activities on Coastal Dunes of the Southern Baltic Sea. *Journal of Coastal Research*, 1145-1157. doi:10.2112/05-0464.1

Hall, C. M. (2001). Trends in ocean and coastal tourism: the end of the last frontier? *Ocean & Coastal Management, 44*(9), 601-618. doi:10.1016/S0964-5691(01)00071-0

Hernández-Calvento, L., Jackson, D. W. T., Medina, R., Hernández-Cordero, A. I., Cruz, N., & Requejo, S. (2014). Downwind effects on an arid dunefield from an evolving urbanised area. *Aeolian Research, 15*, 301-309. doi:10.1016/j.aeolia.2014.06.007

Hersen, P. (2005). Flow effects on the morphology and dynamics of aeolian and subaqueous barchan dunes. *Journal of Geophysical Research: Earth Surface, 110*(F4). doi:10.1029/2004JF000185

Hesp, P. A. (1989). A review of biological and geomorphological processes involved in the initiation and development of incipient foredunes. *Proceedings of the Royal Society of Edinburgh, Section B: Biological Sciences, 96*, 181-201.

Hoonhout, B. (2017). *Aeolian Sediment Availability and Transport.* Technical University Delft, Delft.

Hoonhout, B. M., & Van Thiel de Vries, J. (2013). *Invloed van strandbebouwing op zandverstuiving, Adviezen voor vergunningverlening*. Delft: Deltares.

Hoonhout, B. M., & Waagmeester, N. (2014). *Invloed van strandbebouwing op zandverstuiving, Een verkenning naar methoden, meetgegevens en modellen*. Delft: Deltares.

Horikawa, K., Hotta, S., Kubota, S., & Katori, S. (1983). On the sand transport rate by wind on a beach. *Coastal Engineering in Japan, 26*(1), 101-120.

Horn, D. P. (2002). Beach groundwater dynamics. *Geomorphology, 48*(1), 121-146. doi:10.1016/S0169-555X(02)00178-2

Houser, C., Labude, B., Haider, L., & Weymer, B. (2013). Impacts of driving on the beach: Case studies from Assateague Island and Padre Island National Seashores. *Ocean & Coastal Management, 71*, 33-45. doi:10.1016/j.ocecoaman.2012.09.012

Hsu, S. A. (1971). Measurement of Shear Stress and Roughness Length on a Beach. *Journal of Geophysical Research, 76*(12), 2880-&. doi:10.1029/JC076i012p02880

Huisman, M. (2013). *De effecten van strandbebouwing op de ontwikkeling van de eerste duinenrij - Evaluatie en advies monitoringsprogramma HHNK (MSc. Thesis).* VU Amsterdam, Amsterdam.

Hulscher, S. J. M. H., & Dohmen-Janssen, C. M. (2005). Introduction to special section on Marine Sand Wave and River Dune Dynamics. *Journal of Geophysical Research: Earth Surface, 110*(F4). doi:10.1029/2005JF000404

Hunt, J. (1971). The effect of single buildings and structures. *Phil. Trans. R. Soc. Lond. A, 269*(1199), 457-467.

Hunt, J. C. R., Abell, C. J., Peterka, J. A., & Woo, H. (1978). Kinematical studies of the flows around free or surface-mounted obstacles; applying topology to flow visualization. *Journal of Fluid Mechanics, 86*(1), 179-200. doi:10.1017/S0022112078001068

Iversen, J. D., Pollack, J. B., Greeley, R., & White, B. R. (1976). Saltation threshold on Mars: The effect of interparticle force, surface roughness, and low atmospheric density. *Icarus, 29*(3), 381-393. doi:10.1016/0019-1035(76)90140-8

Iversen, J. D., & White, B. R. (1982). Saltation Threshold on Earth, Mars and Venus. *Sedimentology, 29*(1), 111-119. doi:DOI 10.1111/j.1365-3091.1982.tb01713.x

Jackson, N. L., & Nordstrom, K. F. (2011). Aeolian sediment transport and landforms in managed coastal systems: A review. *Aeolian Research, 3*(2), 181-196. doi:10.1016/j.aeolia.2011.03.011

Keijsers, J. (2015). *Modelling foredune dynamics in response to climate change.* Wageningen University.

Kok, J. F., Parteli, E. J., Michaels, T. I., & Karam, D. B. (2012). The physics of wind-blown sand and dust. *Rep Prog Phys, 75*(10), 106901. doi:10.1088/0034-4885/75/10/106901

Liu, M., Zhang, Q., Fan, F., & Shen, S. (2018). Experiments on natural snow distribution around simplified building models based on open air snow-wind combined experimental facility. *Journal of Wind Engineering and Industrial Aerodynamics, 173*, 1-13. doi:10.1016/j.jweia.2017.12.010

Livingstone, I., Wiggs, G. F. S., & Weaver, C. M. (2007). Geomorphology of desert sand dunes: A review of recent progress. *Earth-Science Reviews, 80*(3), 239-257. doi:10.1016/j.earscirev.2006.09.004

Malavasi, M., Santoro, R., Cutini, M., Acosta, A. T. R., & Carranza, M. L. (2013). What has happened to coastal dunes in the last half century? A multitemporal coastal landscape analysis in Central Italy. *Landscape and Urban Planning, 119*, 54-63. doi:10.1016/j.landurbplan.2013.06.012

Malvarez, G., Jackson, D., Navas, F., Bilbao, I., & Hernández-Calvento, L. (2013). *A Conceptual Model for Dune Morphodynamics of the Corralejo Dune System, Fuerteventura, Spain* (Vol. SI 65).

Martinuzzi, R., & Tropea, C. (1993). The Flow Around Surface-Mounted, Prismatic Obstacles Placed in a Fully Developed Channel Flow (Data Bank Contribution). *Journal of Fluids Engineering, 115*(1), 85-92. doi:10.1115/1.2910118

McLeod, E. M., Guay, P.-J., Taysom, A. J., Robinson, R. W., & Weston, M. A. (2013). Buses, Cars, Bicycles and Walkers: The Influence of the Type of Human Transport on the Flight Responses of Waterbirds. *PLOS ONE, 8*(12), e82008. doi:10.1371/journal.pone.0082008

Meroney, R. N., Leitl, B. M., Rafailidis, S., & Schatzmann, M. (1999). Wind-tunnel and numerical modeling of flow and dispersion about several building shapes. *Journal of Wind Engineering and Industrial Aerodynamics, 81*(1), 333-345. doi:10.1016/S0167-6105(99)00028-8

Mitteager, W., Burke, A., & Nordstrom, K. (2006). Restoring natural landscapes on private shorefront properties in New Jersey, USA. *Journal of Coastal Research*, 890-897.

Moffett, M. D., McLachlan, A., Winter, P. E. D., & De Ruyck, A. M. C. (1998). Impact of trampling on sandy beach macrofauna. *Journal of Coastal Conservation, 4*(1), 87-90. doi:10.1007/bf02806494

Moreno, A., & Amelung, B. (2009). Climate Change and Coastal & Marine Tourism: Review and Analysis. *Journal of Coastal Research*, 1140-1144.

Morton, R. A., Paine, J. G., & Gibeaut, J. C. (1994). Stages and Durations of Post-Storm Beach Recovery, Southeastern Texas Coast, USA. *Journal of Coastal Research, 10*(4), 884-908.

Namikas, S. L., & Sherman, D. J. (1995). A Review of the Effects of Surface Moisture Content on Aeolian Sand Transport. In V. P. Tchakerian (Ed.), *Desert Aeolian Processes* (pp. 269-293). Dordrecht: Springer Netherlands.

NASA. (2002). City-swallowing Sand Dunes. Retrieved from https://science.nasa.gov/science-news/science-at-nasa/2002/06dec_dunes

Nickling, W. (1988). The initiation of particle movement by wind. *Sedimentology, 35*(3), 499-511.

Nordstrom, K., McCluskey, J., & Rosen, P. (1986). Aeolian processes and dune characteristics of a developed shoreline: Westhampton Beach, New York. *Aeolian geomorphology*, 131-147.

Nordstrom, K. F. (2000). *Beaches and dunes of developed coasts*: Cambridge University Press.

Nordstrom, K. F., & Arens, S. M. (1998). The role of human actions in evolution and management of foredunes in The Netherlands and New Jersey, USA. *Journal of Coastal Conservation, 4*(2), 169-180. doi:10.1007/bf02806509

Nordstrom, K. F., & Jackson, N. L. (1998). Effects of a high rise building on wind flow and beach characteristics at Atlantic City, NJ, USA. *Ocean & Coastal Management, 39*(3), 245-263. doi:10.1016/S0964-5691(97)00036-7

Nordstrom, K. F., Jackson, N. L., Korotky, K. H., & Puleo, J. A. (2011). Aeolian transport rates across raked and unraked beaches on a developed coast. *Earth Surface Processes and Landforms, 36*(6), 779-789. doi:10.1002/esp.2105

Nordstrom, K. F., & James, M. M. (1985). The Effects of Houses and Sand Fences on the Eolian Sediment Budget at Fire Island, New York. *Journal of Coastal Research, 1*(1), 39-46.

Nordstrom, K. F., & McCluskey, J. M. (1984). Considerations for control of house construction in coastal dunes. *Coastal Management, 12*(4), 385-402.

Oikawa, S., & Tomabechi, T. (2000). Daily observations of snowdrifts around a model cube. *Fourth Conference of Snow Engineering*, 137-141.

Peterka, J. A., Meroney, R. N., & Kothari, K. M. (1985). Wind flow patterns about buildings. *Journal of Wind Engineering and Industrial Aerodynamics, 21*(1), 21-38. doi:10.1016/0167-6105(85)90031-5

Province of Noord-Holland. (2017). *Toekomstperspectief 2040 Noord-Hollandse Noordzeekust, ruimte voor rust en reuring*.

Ranieri, L. A. (2014). *Morfodinâmica costeira e o uso da orla oceânica de Salinópolis (Nordeste do Pará).* (Doctoral degree Doctoral thesis), Universidade Federal do Pará, Belém.

Reinders, J., Van der Valk, B., & Van der Meulen, F. (2014). *Effecten van tijdelijke strandbebouwing op de ontwikkeling van de jonge zeereep (H2130: Wit Duin) aan de zeezijde van de Duincompensie Delfstandse Kust (1206682-000-ZKS-0014)*. Delft: Deltares.

Rice, M. A., Willetts, B. B., & McEwan, I. K. (1996). Observations of collisions of saltating grains with a granular bed from high-speed cine-film. *Sedimentology, 43*(1), 21-31. doi:10.1111/j.1365-3091.1996.tb01456.x

Rickard, C. A., McLachlan, A., & Kerley, G. I. H. (1994). The effects of vehicular and pedestrian traffic on dune vegetation in South Africa. *Ocean & Coastal Management, 23*(3), 225-247. doi:10.1016/0964-5691(94)90021-3

Schlacher, T. A., Schoeman, D. S., Dugan, J., Lastra, M., Jones, A., Scapini, F., & McLachlan, A. (2008). Sandy beach ecosystems: key features, sampling issues, management challenges and climate change impacts. *Marine Ecology, 29*(s1), 70-90. doi:10.1111/j.1439-0485.2007.00204.x

Schlacher, T. A., Thompson, L., & Price, S. (2007). Vehicles versus conservation of invertebrates on sandy beaches: mortalities inflicted by off-road vehicles on ghost crabs. *Marine Ecology, 28*(3), 354-367. doi:10.1111/j.1439-0485.2007.00156.x

Schlacher, T. A., & Thompson, L. M. C. (2008). Physical Impacts Caused by Off-Road Vehicles to Sandy Beaches: Spatial Quantification of Car Tracks on an Australian Barrier Island. *Journal of Coastal Research, 24*(sp2), 234-242, 239.

Schulman, L. L., Strimaitis, D. G., & Scire, J. S. (2000). Development and Evaluation of the PRIME Plume Rise and Building Downwash Model. *Journal of the Air & Waste Management Association, 50*(3), 378-390. doi:10.1080/10473289.2000.10464017

Shao, Y., & Raupach, M. (1992). The overshoot and equilibration of saltation. *Journal of Geophysical Research: Atmospheres, 97*(D18), 20559-20564.

Shao, Y. P., & Lu, H. (2000). A simple expression for wind erosion threshold friction velocity. *Journal of Geophysical Research-Atmospheres, 105*(D17), 22437-22443. doi:10.1029/2000jd900304

Shields, A. (1936). Anwendung der Aehnlichkeitsmechanik und der Turbulenzforschung auf die Geschiebebewegung. *PhD Thesis Technical University Berlin*.

Smith, A. B., Jackson, D. W. T., & Cooper, J. A. G. (2017a). Three-dimensional airflow and sediment transport patterns over barchan dunes. *Geomorphology, 278*, 28-42. doi:10.1016/j.geomorph.2016.10.025

Smith, A. B., Jackson, D. W. T., Cooper, J. A. G., & Hernández-Calvento, L. (2017b). Quantifying the role of urbanization on airflow perturbations and dunefield evolution. *Earth's Future, 5*(5), 520-539. doi:10.1002/2016ef000524

Taylor, P. A. (1969). On wind and shear stress profiles above a change in surface roughness. *Quarterly Journal of the Royal Meteorological Society, 95*(403), 77-91. doi:10.1002/qj.49709540306

Thiis, T., & Jaedicke, C. (2000). *The snowdrift pattern around two cubical obstacles with varying distance, measurements and numerical simulations.* Paper presented at the Snow Engineering: Recent Advances and Developments. Proceedings of the Fourth International Conference on Snow Engineering. Norwegian University of Science and Technology.

Thiis, T. K. (2003). Large scale studies of development of snowdrifts around buildings. *Journal of Wind Engineering and Industrial Aerodynamics, 91*(6), 829-839. doi:10.1016/S0167-6105(02)00474-9

Thiis, T. K., & Gjessing, Y. (1999). Large-scale measurements of snowdrifts around flat-roofed and single-pitch-roofed buildings. *Cold Regions Science and Technology, 30*(1), 175-181. doi:10.1016/S0165-232X(99)00021-X

Tsoar, H. (1983). *Wind Tunnel Modeling of Echo and Climbing Dunes* (Vol. 38).

Tsoar, H., & Blumberg, D. (1991, 1991//). *The effect of sea cliffs on inland encroachment of aeolian sand.* Paper presented at the Aeolian Grain Transport, Vienna.
Ungar, J. E., & Haff, P. K. (1987). Steady state saltation in air. *Sedimentology, 34*(2), 289-299.
Van Beeck, J., Conan, B., & Planquart, P. (2011). *Windtunnelproeven ter bepaling van het effect van strandhuisjes op het zandtransport bij Slag Vluchtenburg*. Retrieved from Sint-Genesius-Rode:
Van der Putten, W. H., Van Dijk, C., & Peters, B. A. M. (1993). Plant-specific soil-borne diseases contribute to succession in foredune vegetation. *Nature, 362*, 53. doi:10.1038/362053a0
Van der Valk, B., & Van der Meulen, F. (2013). *Ecologisch en morfologisch advies strandbebouwing. Memo 30 juli 2013*. Delft: Deltares.
Van der Wal, D. (1998). The impact of the grain-size distribution of nourishment sand on aeolian sand transport. *Journal of Coastal Research*, 620-631.
Van Onselen, E. P. (2018). *Analysing measures to improve beach-dune interaction in the presence of man-made structures using computational fluid dynamics (CFD)*. Retrieved from Utrecht:
Van Puijenbroek, M. E. B. (2017). *Dunes, above and beyond : the interactions between ecological and geomorphological processes during early dune development.* (Includes bibliographical references. - With summaries in English and Dutch), Wageningen University, Wageningen.
Van Puijenbroek, M. E. B., Limpens, J., De Groot, A. V., Riksen, M. J. P. M., Gleichman, M., Slim, P. A., . . . Berendse, F. (2017). Embryo dune development drivers: beach morphology, growing season precipitation, and storms. *Earth Surface Processes and Landforms, 42*(11), 1733-1744. doi:10.1002/esp.4144
Wang, H. F., & Zhou, Y. (2009). The finite-length square cylinder near wake. *Journal of Fluid Mechanics, 638*, 453-490. doi:10.1017/S0022112009990693
Weston, M. A., Schlacher, T. A., & Lynn, D. (2014). Pro-Environmental Beach Driving is Uncommon and Ineffective in Reducing Disturbance to Beach-Dwelling Birds. *Environmental Management, 53*(5), 999-1004. doi:10.1007/s00267-014-0256-4
Wiggs, G. F. S., Livingstone, I., & Warren, A. (1996). The role of streamline curvature in sand dune dynamics: evidence from field and wind tunnel measurements. *Geomorphology, 17*(1), 29-46. doi:10.1016/0169-555X(95)00093-K
Williams, A., & Feagin, R. (2010). Sargassum as a Natural Solution to Enhance Dune Plant Growth. *Environmental Management, 46*(5), 738-747. doi:10.1007/s00267-010-9558-3
Williams, I. A., Wijnberg, K. M., & Hulscher, S. J. M. H. (2018). Detection of aeolian transport in coastal images. *Aeolian Research, 35*, 47-57. doi:10.1016/j.aeolia.2018.09.003
Wilson, D. J. (1979). Flow patterns over flat roofed buildings and application to exhaust stack design. *ASHRAE Trans., 85*, 284-295.
Witmer, A. D., & Roelke, D. L. (2014). Human interference prevents recovery of infaunal beach communities from hurricane disturbance. *Ocean & Coastal Management, 87*, 52-60. doi:10.1016/j.ocecoaman.2013.11.005
Yalin, M. S., & Karahan, E. (1979). Inception of Sediment Transport. *Journal of the Hydraulics Division-Asce, 105*(11), 1433-1443.
Zingg, A. (1953). *Wind tunnel studies of the movement of sedimentary material.* Paper presented at the Proceedings of the 5th Hydraulic Conference Bulletin.